Results in Engineering 30 (2026) 110562

Contents lists available at ScienceDirect

Results in Engineering

journal homepage: www.sciencedirect.com/journal/results-in-engineering

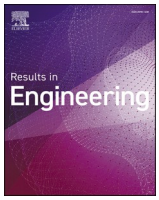

Research paper

Performance of styrene-butadiene-rubber modified bitumen for sustainable pavement constructions in tropical regions

Daniel Akinmade [b,c,*], Adesola Afolabi [a,b], Adekunle A. Adeleke [d], Samson Duna [b], Mario Sandor [e], Kumar Anupam [c]

[a] Department of Civil Engineering, Faculty of Engineering, Nile University of Nigeria, Abuja, Nigeria
[b] Nigerian Building and Road Research Institute, NBRRI House/I.T. Igbani Street, Jabi, Abuja, Nigeria
[c] Faculty of Civil Engineering & Geosciences, Delft University of Technology, Stevinweg 1, Delft, 2628 CN, the Netherlands
[d] Department of Mechanical Engineering, Faculty of Engineering, Nile University of Nigeria, Abuja, Nigeria
[e] BASF SE Carl-Bösch-Str. 38, 67056, Ludwigshafen, Germany

ARTICLE INFO

Keywords:
SBR
Polymer-modified bitumen
Rutting resistance
Fatigue
Tropical pavements

ABSTRACT

Pavements in tropical regions are affected by high temperatures and ageing, and are susceptible to rutting, which reduces their resilience and durability. Hence, this study investigates the modification of bitumen with Styrene–Butadiene Rubber (SBR) at 0%, 3%, 6%, and 9% by weight. Conventional tests showed that SBR modification improved high-temperature properties up to 6%, followed by a sudden reduction at 9% modification, as evidenced by increased softening point and reduced penetration. At 6% modification, the SBR-modified bitumen would remain uniform and stable during storage. It would not affect performance upon use after storage, demonstrating its suitability as a performance-enhancing polymer for hot-climate applications. Multiple Stress Creep Recovery (MSCR) testing shows reductions in non-recoverable creep compliance and enhanced elastic recovery, making the modified bitumen. The 6% SBR modified binder showed a significantly higher Jnr diff value with a Jnr diff value of 53.42%. Similarly, the SBR-modified binders showed improved recovery, with %R 0.1 values of 14.89% to 18.45% at 64 °C and %R 3.2 values of 0.32% to 1.71%. Linear Amplitude Sweep (LAS) results showed that a 9% modification yielded the highest N_f value, but beyond 6%, the improvement was negligible. Considering cost and optimal performance, 6% SBR content modification should be considered. Glover–Rowe parameters showed that SBR-modified binders retained their elasticity and reduced the brittleness of bitumen, unlike unmodified binders, which shifted towards brittle behaviour. Pearson correlation analysis shows a strong positive cluster among fatigue life, % recovery, Fail Temperature (Unaged and Aged), G*/sin δ, softening point, elastic recovery, and rutting parameters, with correlation values exceeding 0.90 in most cases. Grey Relational Analysis (GRA) shows that a 6% SBR with a Grey Relational Grade (GRG) of 0.843 was ranked highest among all modifications. Principal Component Analysis (PCA) shows that a 6% SBR modification of the bitumen is optimal, providing a balance among rutting resistance, fatigue performance, and ageing durability. These findings highlight the potential of SBR-modified bitumen to enhance pavement performance and service life in tropical climates.

1. Introduction

Asphalt pavements are essential components of transport infrastructure that provides links for economic activity and societal well-being [1]. Asphalt pavement is constructed from aggregates of different sizes, typically combined with bitumen at high temperatures. Bitumen, the binding agent is derived from crude oil and is the widely used binder for asphalt pavements on roads, airports and bridge decks [2,3]. Bitumen has been used for industrial purposes long before it was used for asphalt pavements. In the 1800s, bitumen began to be used as a binder for asphalt pavements, first by a Belgian scientist in the United States for road construction [4].

Bitumen is a viscoelastic material that behaves both like a viscous liquid at high temperatures and an elastic material at low temperatures [5,6]. It plays a vital role in modern road pavement construction due to its economic, engineering benefits and its ability to stabilise the

* Corresponding author.
E-mail address: o.d.akinmade@tudelft.nl (D. Akinmade).

https://doi.org/10.1016/j.rineng.2026.110562
Received 6 February 2026; Received in revised form 4 April 2026; Accepted 15 April 2026
Available online 15 April 2026

aggregate skeleton [7]. As the number of automobiles grew, the demand for more and better roads increased, which in turn led to a high demand for quality bitumen [8]. This demand stems from industrial requirements, including the need for roads that can withstand heavy loads and adverse weather. As a result, global demand for bitumen has exceeded 100 million metric tons annually [9-11]. Furthermore, the high demand for bitumen, combined with the increasing frequency of extreme weather events, and rising oil costs has created a need for an alternative bitumen source.

Although researchers have begun to explore other binder sources and sustainable practices to address these issues as highlighted above [12,13] Amongst other sustainable practices, polymer-modified bitumen and asphalt concrete have also gained popularity in pavement construction due to their enhanced engineering properties [14]. Incorporating polymers, bio-oils, crude oil shale, biomass, microalgae, and waste materials into the mixtures at different dosages to serve as modifiers is widely used in order to improve the performance of asphalt concrete [15,16].

Polymer modification of asphalt binders has become a well-established strategy for enhancing pavement performance under demanding traffic and environmental conditions. Among the most widely used modifiers, Styrene-Butadiene-Styrene (SBS), Ethylene-Vinyl-Acetate (EVA), and crumb rubber (CR) have received extensive research attention globally [17]. However, their performance and economic feasibility under tropical climatic conditions remain variable and context-dependent [18]. Typically, conventional polymer-modified bitumen (PMB) contains 3–4.5 % polymer, while highly modified polymer-modified bitumen (PMB) contains 6–7.5 % polymer. However, the interaction between polymer structure and content remains unclear and ambiguous especially in tropical regions [19]. It was also observed that during asphalt mixture production and construction, polymers are susceptible to heat and oxidative degradation [20–22]. Specifically, the unsaturated $C{=}C$ bonds in PB blocks are prone to fracture under thermal oxidative ageing conditions, causing modification effects to degrade or disappear [23,24]. Studies have demonstrated significant degradation of SBS-modified bitumen during short-term ageing. A 60 % decrease in the percent recovery of extracted binders was found after 4 h of short-term ageing at 165 °C [22].

In tropical regions, pavements are typically exposed to aggressive ambient conditions. For example, pavement surface temperatures in West African tropical climates regularly exceed 60 °C during peak solar exposure hours [25,26]. Sustained ultraviolet (UV) radiation and high humidity compound the effects of thermal stress on binder chemistry [27] this would have a corresponding effect on the hot mix asphalt. Past Studies [28] have highlighted that urban microclimates in countries like Nigeria are driven by the complex interaction of incident solar radiation. This interaction with surface materials can generate localised heat-island effects that may necessitate the use of higher-performance-grade binders [25]. These combined stressors significantly influence binder rheology and accelerate oxidative ageing which makes the conventional and even modified binders susceptible to premature distress [29]. Within this context, the performance limitations of commonly used modifiers become particularly relevant. Although SBS-modified asphalt has demonstrated high performance capabilities, it is associated with high cost and poor storage stability [18]. On the other hand, the crumb rubber-modified asphalt suffers from poor workability, segregation issues, limiting their broad applicability in challenging environments [30]. EVA a plastomeric modifier improves rutting resistance and stiffness but lacks the elasticity needed for effective fatigue resistance under repeated loading [31,32].

Styrene-Butadiene Rubber (SBR) is a copolymer that has a molecular structure consisting of styrene and butadiene chain which could enhance the elastomeric mechanism in AC mixtures [33]. Because of this, SBR is reported [34] to improve stiffness, elasticity, and ageing resistance with improved durability. It also lowers cumulative strain compared to unmodified mixtures and ageing resistance with improved durability with lower cumulative strain compared to unmodified mixtures. In Comparison to SBS, SBR offers relatively better storage stability, workability and reduction in practical challenges during mixing and application [35]. Unlike plastomeric modifiers such as EVA, SBR enhances binder flexibility without excessively increasing post-ageing brittleness [32]. Past studies [34] have confirmed that SBR modifiers effectively improve low-temperature rheological performance, and that composite SBR systems can improve overall ageing resistance of binder systems.

Sustainable processes such as recycling asphalt pavement (RAP) are also sustainable practices in the asphalt industry [16]. Researchers [36] used recycled rubber on tire-derived aggregate in the mixtures and they reported that the subgrades exhibited enhanced cracking resistance and higher fracture energy compared with conventional asphalt mixtures. Moreover, field overlays with ground tyre rubber and tyre fabric fibres showed increased rutting and cracking resistance as well as reduced noise, with no cracking evident in post-construction evaluations. Similarly, the use of rubber-modified mixtures with stress-absorbing membrane interlayers has been shown to boost fracture energy and overall pavement performance. This further highlights the functional benefits of rubber modification in hot mix asphalt systems. Concurrently, research has consistently demonstrated the benefits of polymer-modified bitumen as explained elsewhere [37-39], highlighting its enhanced properties [40,41]. Specifically highlighted the effectiveness of Styrene-Butadiene-Styrene in enhancing asphalt performance. Although the influence of polymers on the performance of bitumen is still complex since it is influenced by various factors such as polymer type, concentration, and the specific production processes [19].

Despite benefits of SBR as highlighted in the previous paragraph, there remains a significant scientific gap which limits its execution in practice in temperate regions. To the best authors' knowledge there are limited or no studies on the effect of high-temperature oxidative environments characteristic of tropical climates on SBR modified asphalt. Most studies have focused more on the comparative studies of SBR- and SBS-modified asphalt binders under accelerated environmental ageing of cold-climate, freeze-thaw and UV exposure [35]. The suitability of SBR-modified bitumen under sustained high-temperature and oxidative tropical conditions has not been sufficiently quantified. Understanding the stability and the robustness of modification effects at different polymer contents subjected to tropical weather conditions are also critically important in selection and optimization [42]. Evaluating SBR-modified bitumen under simulated tropical climatic conditions is therefore necessary to determine its suitability for sustainable pavement applications in regions such as Nigeria. To address this research gap, this study investigates the rheological and performance-related properties of SBR-modified bitumen under tropical weather conditions. It is highlighted that the study considers both short- and long-term rheological ageing stability.

2. Objective

This study aims to evaluate the physio-rheological and mechanical performance of styrene-butadiene-rubber (SBR) modified bitumen. The research investigates high-temperature rutting resistance, fatigue behaviour, oxidative ageing susceptibility, and durability performance, with the goal of identifying an optimal modifier dosage to enhance pavement service life.

3. Materials and methods

The following section outlines the methodology and experimental approach used in this research. This includes the sample preparation process, characterisation process, and various test protocols and conditions are presented in the following subsections.

3.1. Sample preparation

Three polymer content levels, 3 %, 6 % and 9 % by mass of the base binder, representing conventional, intermediate and highly modified polymer-modified bitumen (PMB), respectively. These were evaluated for their impact on binder performance, as shown in Fig. 1 below and summary of the test and the number of replicates carried out is presented in Table 1. The polymer was added to the bitumen in drops. and the binder was mixed using a shear mixer at a speed of 3500 rpm for 45mins at a temperature of 155 °$C \pm 5$ °C. Short-term aging of the binders was simulated by a rotating thin film oven (RTFO) test [21,43,44]. Three groups of samples were prepared for each binder, and ageing was carried out at 163 °C with an airflow rate of 4000 mL/min for 85 min. The pressure ageing vessel (PAV) was used to simulate the long-term ageing of asphalt as two sets of RTFO samples were heated to a flowing state in an oven. Subsequently, these 50 g RTFO samples were poured into a PAV pan and aged in the vessel. The ageing temperature, air pressure and ageing time were 100 °C, 2.1 MPa and 20 h, respectively.

3.2. Materials

The materials used in this study include the base binder 60/70 and the SBR modifier.

3.2.1. Base binder

The base binder used in this study was the conventional 60/70 bitumen used in Nigeria and obtained from Gradient Bitumen, one of the leading bitumen companies in Nigeria.

3.2.2. SBR polymer modifier

The SBR polymer used as a modifier in this study is a mechanically stable latex polymer dispersion obtained from BASF West Africa Ltd. The properties of the SBR polymer are shown in Table 2.

Table 1
Conducted laboratory tests on the asphalt binder and modified samples.

Test	Number of replicates
Penetration test	3
Softening point test	3
Ductility	3
Elastic recovery test	3
Cigar tube test	3
Frequency sweep tests	2
Temperature sweep tests	2
Linear amplitude sweep (LAS)	2
Multiple stress creep recovery (MSCR)	2
Glover-Rowe	2

Table 2
Basic properties of SBR polymers.

Physical properties	Values
Visible condition	Aqueous, white to light yellow
Solids content	51 %
Viscosity	1000 mPa•s (Brookfield RVT, Spindle #2, 20 rpm, 23 °C)
Specific gravity	1 g/cm3
pH	7.5

3.3. Index properties

The index properties of the base binder (60/70) and modified binders were conducted using penetration, ductility and softening point following ASTM specifications. To establish the baseline, tests on the physical characteristics of the bitumen were conducted. Although this study focuses on performance-based evaluation hence it was necessary to add these tests to verify the grade and consistency of the base binder and the modified binder. This is to obtain information on the evolution of stiffness and temperature susceptibility at this scale. These index tests

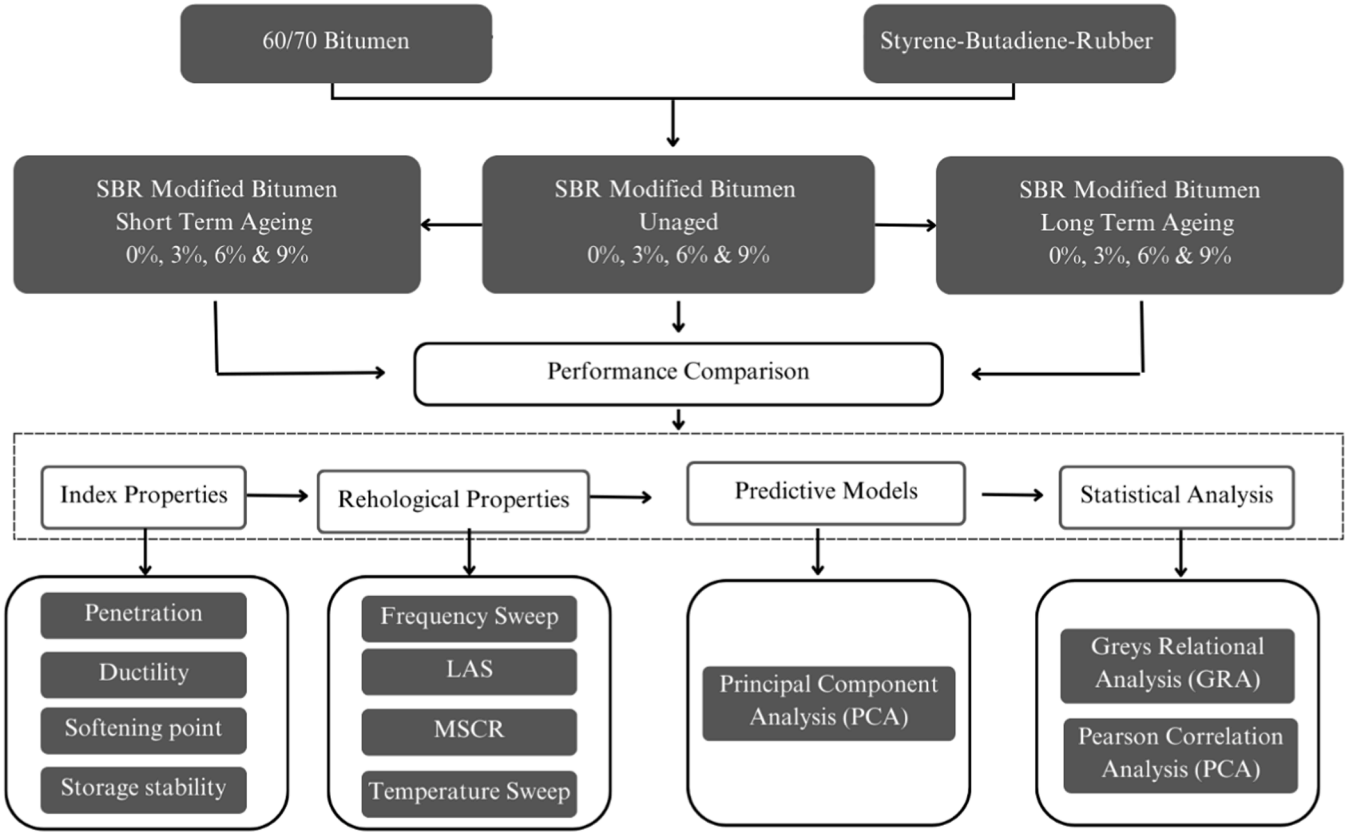

Fig. 1. Schematic experimental flow chart.

provide a preliminary indication of hardening or softening effects induced by modification and serve as an essential reference point for interpreting subsequent performance-based results.

3.3.1. Penetration test

The penetration test was conducted to assess the consistency of the base binder in comparison with the modified binder with SBR at varying percentages. The test was performed by measuring the depth, in millimetres, to which a standard needle, loaded with 100 g, will penetrate vertically in five (5) seconds. This test is conducted at a temperature of 25 °C as outlined in ASTM D5 [45].

3.3.2. Softening point test

The softening point test was conducted to compare the consistency of the base binder and SBR-modified binders. The softening point test was conducted in accordance with EN 1427 [46]. The softening point is the temperature at which the bitumen sample can no longer support the weight of a 3.5 g steel ball and falls through a height of 25 mm. A higher softening point indicates hard bitumen, while a lower softening point indicates soft bitumen.

3.3.3. Ductility and elastic recovery test

The ductility test was conducted to assess the adhesive and plastic properties of the base binder compared with those of the binder modified with SBR. It was carried out by stretching a standard bitumen briquette specimen at a uniform speed of 5 cm per minute in a water bath maintained at 25 °C until the bitumen thread breaks. The distance in centimeters through which the sample stretched before failure was recorded as its ductility value in accordance with ASTM D113 [47]. Similarly, the elastic recovery test was conducted to determine the ability of the modified and base binder to regain their original shape after deformation. Furthermore, during this test the percentage recovery was calculated as specified in ASTM D6084 [47].

3.3.4. Cigar tube test

The cigar tube test was used to evaluate the storage stability of SBR-modified bitumen in accordance as reported elsewhere [48]. The testing procedure involved pouring hot binder into aluminium tubes, as shown Fig. 2 followed by vertical storage in an oven at 163 °C for 48hours. After heating, the cigar tubes were placed in a refrigerator for 4 h and then evenly divided into three parts, in line with established methodologies [49]. Subsequently, the softening points of the binder extracted from the top and bottom of the tube were determined and the resulting values were compared to assess phase separation and compatibility.

3.4. Ageing conditions

The ageing behaviour of the binders was evaluated under three conditions to simulate field oxidative hardening at various service stages. The condition represented the asphalt binder in its virgin state, short-term ageing, and long-term ageing. The short-term ageing was simulated using the Rolling Thin Film Oven (RTFO) test, 35 g of the virgin binder was heated in a rolling thin film oven at 163 °C for 85 min, and an airflow rate of 4000mL/min [50]. The long-term ageing was simulated using the Pressure Ageing Vessel (PAV) test using the RTFO-aged binder. 50 g of the sample was subjected to 100 °C at 2.1 MPa for 20hours in a PAV tray. The samples were evenly spread across the tray, with a maximum thickness of 3.2 mm, in accordance with ASTM D652 [51]. This would mimic the oxidative ageing that occurs during in-service pavement life. These laboratory ageing protocols enabled the comparison of the rheological properties of the base and SBR-modified binders under conditions representing both construction and extended-field exposure.

3.5. Rheological and performance tests

Rheological tests were conducted on SBR-modified asphalt samples to assess their performance characteristics. The rheological test was conducted on both the base binder and the SBR-modified binder to evaluate their performance. The frequency sweep test, performance grade, MSCR, Glover-Rowe (G-R) test and the LAS were conducted for the investigations [52,53]. The following subsections discuss the tests performed under various stress conditions and temperatures providing insights into the rutting and cracking potential of the modified and base binders.

3.5.1. Frequency sweep tests

The frequency sweep test was conducted at intermediate to high temperatures (25 °C and 28 °C-82 °C) in 6 °C increments over a frequency range of 0.1 Hz to 10 Hz. The test was conducted using parallel plates with a diameter of 25.0 mm and a gap of 1.0 mm for temperatures above 40 °C, and parallel plates with a diameter of 8.0 mm and a gap of 2.0 mm for temperatures below 40 °C. To ensure linear viscoelastic (LVE) response, the shear strain amplitude was measured via an amplitude sweep test over a range of 0.01 % to 100 % at 25 °C and 10 Hz. To accurately capture the complex shear modulus and phase angle

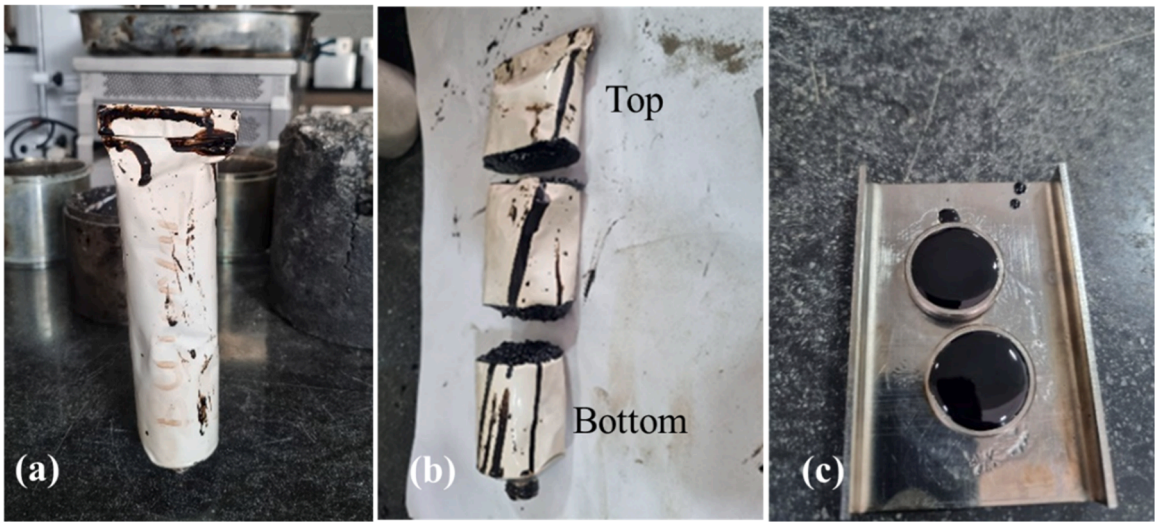

Fig. 2. (a) SBR modified sample in a cigar tube for storage stability test (b) Cigar tube cut into three parts: top, middle, and bottom (c) Sample testing using the ring and ball apparatus.

master curves the sigmoidal model [54] was used. The expression for the sigmoidal model is given by Eq. (1) and Eq. (22).

$$\log|G^*| = \left(v_1 + \frac{\alpha_1}{1 + e^{(\beta_1+\gamma_1 (\log f + \log\alpha(T)))}}\right) \quad (1)$$

$$= \left(-90 \times \alpha_1\gamma_1 \frac{e^{(\beta_1+\gamma_1 (\log f + \log\alpha(T)))}}{[1 + e^{(\beta_1+\gamma_1 (\log f + \log\alpha(T)))}]^2}\right) \quad (2)$$

where G^* is the complex shear modulus, δ is the phase angle, v_1 is the minimum asymptote, α is the difference between maximum and minimum modulus, β is the location parameter that controls the horizontal shift. γ is the shape parameter, f represents the measured frequency (Hz) from DSR test, and a_T is the shift factor. From this test, the master curves of complex shear modulus (G*) and phase angle (δ) were plotted (see Section 4). The cole-cole diagram and black diagram was utilized to characterize the LVE rheological properties of both modified and unmodified bitumen across the frequency and temperature range as explained elsewhere [55].

3.5.2. Temperature sweep test

The temperature sweep test was conducted to evaluate the viscoelastic behaviour of the base binder in comparison to the SBR-modified binders across a range of temperatures in accordance with the standard (ASTM D6373–21a, 2021). From the test, the rutting factor (G*/sin δ) and fatigue cracking factor (G*sin δ) were determined at different temperatures, and the high critical temperature was identified as the point at which the binder transitions to inadequate rutting resistance. Furthermore, two rheological ageing indices were calculated to quantify the effect of oxidative ageing on the binder performance. The Ageing Index used are based on the Fatigue Cracking Factor (AIFCF) and the Ageing Index based on the Rutting Factor (AIRF), as shown Eq. (3) and Eq. (22) respectively [56]. A lower ageing index indicates reduced ageing sensitivity and thus improved resistance to performance loss during long-term service.

$$AI_{FCF} \frac{G^* \times \sin\delta_{aged}}{G^* \times \sin\delta_{unaged}} \quad (3)$$

$$AI_{RF} \frac{G^*/\sin\delta_{aged}}{G^*/\sin\delta_{unaged}} \quad (4)$$

3.5.3. LAS method of analysis

The LAS test was conducted according to standard.(AASHTO TP 101–12) [57] to evaluate the fatigue properties of bitumen. The test determined the fatigue life of the bitumen by measuring its complex modulus (G*) and phase angle (δ) as a function of increasing strain amplitude. The procedure began with measurements LVE range (strain amplitude of 0.1 %) and a temperature of 25 °C over a frequency range of 0.2 - 30 Hz. This was followed by LAS from 0.1 % to 30 % at a constant frequency of 10 Hz and a temperature of 25 °C. The test was conducted using the 8 mm plate geometry and a gap of 2 mm as described in a prior study [58]. The results were then used to provide valuable information on the SBR-modified binder's fatigue resistance, based on Eq. (5) to Eq. (22). The damage accumulation, D(t), of the modified bitumen is expressed using Eq. (5) with respect to the testing time, t [13].

$$D(t) = \sum_{i}^{N} \left[\pi\gamma_o^2 (C_{i-1} - C_i)\right]^{\frac{\alpha}{1+\alpha}} (t_i - t_{i-1})^{\frac{1}{1+\alpha}} \quad (5)$$

where $D_{(t)}$ is the damage accumulation in the specimen, $C_{(i)}$ is the ratio of complex modulus at any time (t) to the initial complex modulus G* (undamaged) $\left\{C_{(t)} = \frac{G^*_t}{G^*_{(initial)}}\right\}$, γ_o is the applied strain for a given data point in percent, t is the testing time in seconds, and $\alpha = \frac{1}{m}$ where m is the slope when the relationship between storage modulus and frequency are characterized by a logarithmic scale plot. By fitting this relationship at any given time, the values of $C_{(t)}$ and $D_{(t)}$ can be accurately obtained, providing valuable insights into the viscoelastic behavior of the material.

$$C_{(t)} = C_O - C_1 D_{(t)}^{C_2} \quad (6)$$

The damage accumulation model is characterized by several key parameters, including C_0, which is set to an initial value of 1, C_1 and C_2, which are curve-fit coefficients derived through linearization of the power law. A critical parameter in evaluating binder fatigue performance is the value of damage accumulation at failure, D_f, which corresponds to the initial complex shear modulus reduction at peak shear stress. This value can be computed using Eq. (7). Eq. (8) provides a quantitative measure of the binder's fatigue performance.

$$D_f = \left(\frac{C_o - C_{peak\ stress}}{C_1}\right)^{\frac{1}{C_2}} \quad (7)$$

$$N_f = A(\gamma_{max})^{-B} \quad (8)$$

and N_f is the fatigue life at 35 % reduction in stiffness as described elsewhere [57].

$A = \frac{f(D_f)^{1+(1-C_2)\alpha}}{(1+(1-C_2)\alpha)\ X\ (\pi C_1 C_2)^{\alpha}}$, $B = 2\alpha$, γ_{max} is the expected maximum strain in percent, and f is the loading frequency at 10 Hz.

3.5.4. MSCR method of analysis

The MSCR test was conducted following AASHTO TP 70–10 [59] specification to evaluate the recovery properties of the modified binder and the base binder. The test was performed at four temperatures (64 °C, 70 °C, 76 °C, and 82 °C) using a 25 mm geometry and 1 mm gap. This is to assess the resistance of the binders to permanent deformation and creep under multiple stress levels. Two distinct stress levels of 0.1 kPa and 3.2 kPa, were applied successively for 10 cycles each, simulating varying traffic loading conditions. The test will meticulously characterise the recovery and non-recovery properties of the bitumen, including percent recovery (%R), non-recoverable creep compliance (Jnr), and stress sensitivity (Jnr *diff*.). These are all critical parameters for evaluating rutting potential in Hot Mix Asphalt (HMA) [60]. The percent recovery was computed using Eq. (9), Jnr was computed using Eq. (10) and the (Jnr *diff*) was computed using Eq. (11) [61]. This detailed assessment provides valuable insights into bitumen performance under shear creep load, informing optimal binder selection and mix design for enhanced pavement durability [62].

$$\%R = \frac{1}{10}\sum_{1}^{10}\left(\frac{(\varepsilon_c - \varepsilon_0) - (\varepsilon_r - \varepsilon_0)}{\varepsilon_c - \varepsilon_0} \times 100\right) \quad (9)$$

$$\text{Jnr} = \frac{1}{10}\sum_{1}^{10}\left(\frac{(\varepsilon_r - \varepsilon_0)}{\sigma}\right) \quad (10)$$

$$\text{Jnr}_{diff} = \frac{Jnr\ 3.2 - Jnr0.1}{Jnr0.1} \times 100 \quad (11)$$

where ε_0 is the Stress before the creep, ε_c is the stress recorded after the 1-second creep, and ε_r is the stress recorded after the 9-seconds recovery.

3.5.5. Glover-Rowe

The cracking susceptibility of the binders was evaluated using the Glover–Rowe (G–R) parameter at 15 °C and 0.005rad/s [63] This specifically combines temperature–frequency to characterize binder embrittlement and ductility loss associated with oxidative ageing. The selected frequency (0.005rad/$s \approx 0.0008$ Hz) represents extremely slow loading conditions, simulating long-term thermal contraction and stress relaxation phenomena that govern crack initiation in aged binders. The reference temperature of 15 °C provides a standardised intermediate

condition at which the binder's viscoelastic balance (stiffness and elasticity) is highly sensitive to ageing-induced structural changes. It is conducted to assess the long-term cracking susceptibility of the base binder in comparison to the SBR-modified binders at different percentages [64]. The test was performed using frequency sweep data obtained from DSR where the complex modulus (G^*) and phase angle (δ) of the binder were measured over a range of temperatures and loading frequencies from 5 °C to 25 °C and 0.1–100rad/s respectively.

The GR-parameter was then calculated using Eq. (12), evaluated at a frequency of 0.005 rad/s with a reference temperature of 15 °C. This temperature is the benchmark for an intermediate condition at which the binder's viscoelastic balance (stiffness and elasticity) is highly sensitive to ageing. Although tropical pavements are primarily exposed to high service temperatures, intermediate-temperature cracking remains a critical distress mechanism due to diurnal cooling cycles and long-term oxidative hardening. Therefore, the G–R parameter at 15 °C enables assessment of embrittlement potential under slow relaxation conditions relevant to field ageing, even in tropical climates. According to established criteria, binders with G-R values exceeding 180 kPa indicate progressive loss of relaxation capability. While values approaching or exceeding 450–480 kPa correspond to severe embrittlement and high cracking probability of the binder [65]. The procedure was carried out in line with the recommendations of the AASHTO TP 10 [58] protocol for determining the LVE properties of asphalt binders.

$$G - R = G^*.\frac{\cos^2\delta}{\sin\delta} \tag{12}$$

3.6. Statistical analysis

To select the optimal modification in the base binder statistical analytical tools were employed based on different performance indicators. The principal component analysis (PCA) was used to identify the most influential indicators. While greys relational analysis (GRA) used the most relevant indicators to rank the binders based on the sensitivity of these indicators and their influence on the binders. Pearsons correlation analysis (PC) was used to measure the strength of the linear relationship between individual indicators during the test. The following subsections would discuss in detail the statistical tools as highlighted.

3.6.1. PCA method of evaluation

PCA evaluation method was applied as a multivariate statistical technique to reduce the dimensionality of the dataset while retaining the original information [66]. This approach was used to identify the most influential performance indicators among the index and rheological properties evaluated in this study and to eliminate redundancy caused by inter-correlated variables. The PCA procedure followed in this research comprised four stages: standardization of data, development of the covariance matrix, extraction of eigenvalues and eigenvectors, and determination of principal components. In the first stage, all experimental data were standardized to reduce the effect of differing measurement scales. The standardized values were obtained using Eq. (13).

$$Z_{ij} = \frac{x_{ij} - \overline{x}_j}{s_j} \tag{13}$$

where x_{ij} is the observed value of the j^{th} variable for the i^{th} experiment, $\overline{x}_j$ is the mean of variable j, and s_j is the standard deviation of variable j. In the second stage, a covariance matrix was constructed to evaluate the correlation structure among the standardized variables, as expressed in Eq. (14).

$$C = \frac{1}{n-1}Z^TZ \tag{14}$$

where C is the covariance matrix of order $p \times p$, with p representing the number of variables.

In the third stage, eigenvalues (λ) and eigenvectors (v) of the covariance matrix were extracted by solving Eq. (15).

$$C_v = \lambda_v \tag{15}$$

The eigenvalues represent the variance explained by each principal component, while the eigenvectors provide the loadings, i.e., the contribution of each variable to a given component. In the fourth stage, the principal components were constructed as linear combinations of the standardised variables, as shown in Eq. (16).

$$PC_j = a_{j1}Z_1 + a_{j2}Z_2 + \ldots + a_{jp}Z_p \tag{16}$$

where PC_j is the j^{th} principal component, and a_{jp} are the loading coefficients derived from the eigenvectors of the j^{th} principal component. Finally, the variance explained by each principal component was computed using Eq. (17).

$$PC_j = \frac{\lambda_j}{\sum_{i=1}^{p}\lambda_i} \times 100 \tag{17}$$

Principal components were ranked by their eigenvalues, and only those that accounted for the most cumulative variance (≥90 %) were retained for interpretation. This ensured that the reduced set of principal components adequately represented the original dataset.

3.6.2. Grey's relational analysis

GRA was employed as a multi-response optimisation tool to evaluate the combined effect of the modifiers on the performance of the asphalt binders [67]. This approach allowed for the simultaneous consideration of multiple performance indicators, thereby converting them into a single relational grade for decision-making. For this study, the procedure was carried out in three phases: the data preprocessing, the determination of the grey relational coefficient, and the calculation of the GRG [68]. In the first stage, the experimental results for each performance indicator were normalised to produce comparable sequences, eliminating dimensional inconsistencies and bringing the values into a comparable 0 to 1 range. The choice of normalisation formula was based on the desired performance objective: larger-the-better based on Eq. (18), smaller-the-better based on Eq. (19).

$$X_i^*(k) = \frac{X_i(k) - minX_i(k)}{maxX_i(k) - minX_i(k)} \tag{18}$$

$$X_i^*(k) = \frac{maxX_i(k) - X_i(k)}{maxX_i(k) - minX_i(k)} \tag{19}$$

where $X_i(k)$ is the actual performance value of the i^{th} experiment for the k^{th} response, $X_i^*(k)$ is the normalized value. In the second stage, the (GRC) was computed to quantify the closeness of each experimental result to the ideal normalized reference sequence. The GRC was calculated using Eq. (20):

$$\xi_i(k) = \frac{\Delta_{min} + \zeta\Delta_{max}}{\Delta_i(k) + \zeta\Delta_{max}} \tag{20}$$

where $\Delta_i(k) = \left|X_0^*(k) - X_i^*(k)\right|$ is the absolute difference between the reference sequence and the normalized sequence, Δ_{min} and Δ_{max} are the minimum and maximum values of all absolute differences, and ζ is the distinguishing coefficient, taken as 0.5 in this study. In the final stage, the GRG was obtained as the average of the GRCs across all performance indicators for each experiment, as given in Eq. (21)

$$\gamma_i = \frac{1}{n}\sum_{k=1}^{n}\xi_i(k) \tag{21}$$

where γ_i is the GRG for the i^{th} experiment, $\xi_i(k)$ is the GRC for the k^{th} response, and n is the total number of performance indicators consid-

ered. The GRG values were then used to rank the experimental trials, with higher grades indicating better overall performance across the selected indicators. The trial condition with the maximum GRG was identified as the optimal binder modification level.

3.6.3. PC method of analysis

PC was employed to evaluate the degree of linear association among the relevant performance indicators considered in this study [69]. This statistical tool was applied to determine whether changes in one performance indicator were systematically related to changes in another. The correlation coefficient (r) quantifies the strength and direction of this relationship and ranges from -1 to +1 [70]. A positive value of r indicates that the two performance indicators increase or decrease together. In contrast, a negative value of r indicates that an increase in one corresponds to a decrease in the other. and zero indicates no linear relationship between the two variables. The PC coefficient is gotten using Eq. (22).

$$r = \frac{\sum (x_i - \overline{x})(y_i - \overline{y})}{\sqrt{\sum (x_i - \overline{x})^2 \sum (y_i - \overline{y})}} \quad (22)$$

where x_i and y_i are individual data points for the two variables, $\overline{x}$ and $\overline{y}$ are the means.

4. Results and discussions

The following subsection discusses the performance of modified bitumen using SBR and the implications for the rheological structures of the modification.

4.1. Base binder

Table 3, present the base binder is a 60/70 with a penetration value of 66 which is within the acceptable limits as specified in the specifications for road construction in Nigeria [71].

4.2. Index properties of SBR modified bitumen

The effect of SBR on the base binder was observed to stiffen the bitumen hence reducing the penetration value and increasing the softening point temperature as shown in Fig. 3.

It was also shown that at 9 %, a change in trajectory was noticed, causing the bitumen to become softer. This indicates that the modified bitumen at 6 % SBR has a greater resistance to temperature, which is an early indication of improved rutting resistance.

4.3. Rheological and performance properties

Modified bitumen exhibits rheological properties like those of unmodified bitumen and is used in various applications, such as road construction. Subsequently, we would focus more on viscoelastic behaviour to describe their performance using SBR.

4.3.1. Linear viscoelastic complex modulus and phase angle master curves

The viscoelastic properties of the base bitumen and SBR-modified

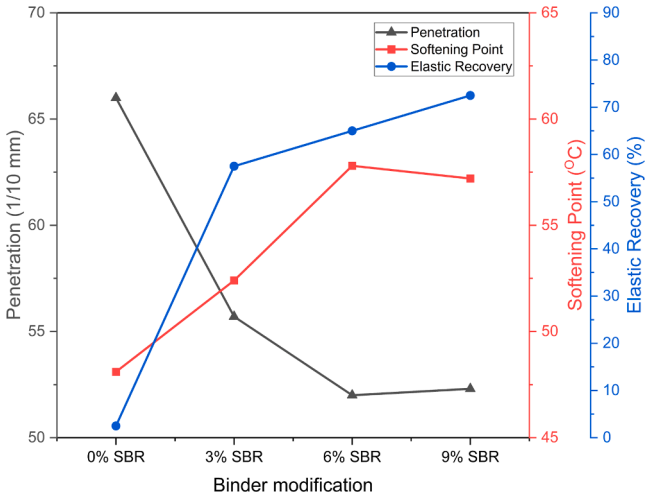

Fig. 3. Effect of SBR dosages (%) on index properties.

bitumen were characterised using a dynamic shear rheometer (DSR). This was examined in their original state through frequency sweep tests at individual strain levels to ensure that the material stays within the linear viscoelastic region as shown in Table 4. The complex modulus master curve was established for SBR-modified bitumen at a reference temperature of 40 °C to simulate the average pavement temperature in Nigeria. The resulting master curves in Fig. 4 to Fig. 7 provides a comprehensive representation of the material's viscoelastic behaviour over a wide range of temperatures and frequencies, by applying Eq. (23) and Eq. (24) with results shown in Figs. 7 and 8.

$$\log a_T = \frac{-C_1(T - T_0)}{C_2 + (T - T_0)} \quad (23)$$

$$\log f_r = \log f + \log a_T = \log f + \frac{-C_1(T - T_0)}{C_2 + (T - T_0)} \quad (24)$$

where: α_T represents the shift factor, T represents the test temperature (°C), C_1 and C_2 are constants obtained and presented in Table 5, T_0 represents the reference temperature (40 °C), f_r represents the reduced frequency (Hz), f represents the measured frequency (Hz).

The complex shear modulus master curves of the SBR modified samples, with a reference temperature of 40 °C, were constructed over a wide range of frequencies, as shown in Fig. 8. In the low-frequency (high-temperature) region, the complex modulus of the base binder increased significantly with the addition of SBR, while the phase angle declined relatively significantly. This suggests that SBR can enhance the high-temperature properties of the base binder, particularly at 6 %; however, at a higher dosage of SBR (9 %), the G* values gradually reduce as the phase angle(δ) increases.

This behaviour could be attributed to the trajectory change in 9 % SBR, as observed in the index properties, which reduced its overall stiffness. In contrast, the high-frequency (low-temperature) region revealed that SBR did not significantly improve the complex modulus of the base binder, as compared to the low-frequency (high-temperature) region, only a slight reduction in stiffness was observed. Also, its phase angle (δ) decreased, indicating that SBR made the base binder slightly

Table 3
Index properties of the base binder.

Parameters	Result	Compliance
Penetration @ 25 °C	66	ASTM D-0005
Softening point (°C)	48.1	ASTM D-36
Elastic Recovery (%)	2.5	ASTM D-6084
Ductility (mm)	>100	ASTM D-113
Flash point (°C)	>300	ASTM D-0092
Specific gravity (g/cm^3)	1.03	ASTM D70

Table 4
Amplitude strain of modified and unmodified binder.

Binder	Amplitude strain
0 % SBR	0.06 %
3 % SBR	0.04 %
6 % SBR	0.03 %
9 % SBR	0.03 %

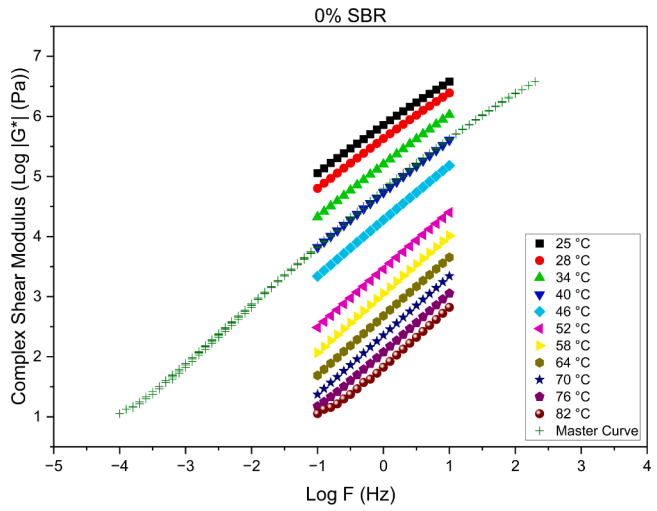

Fig. 4. Frequency sweep for 0 % modification at reference temperature of 40 °C.

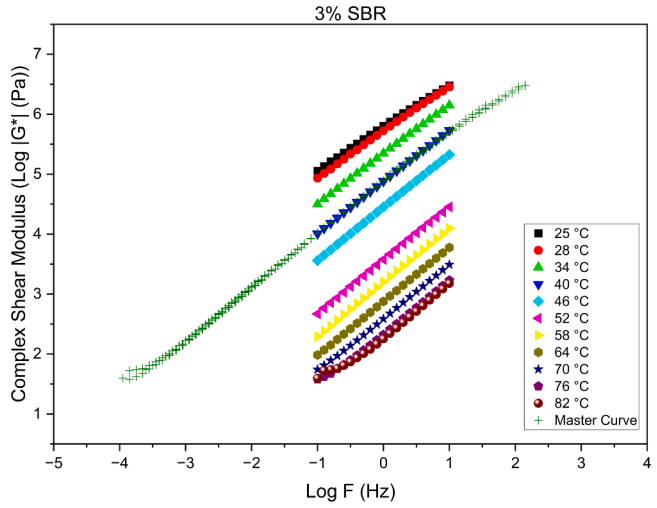

Fig. 5. Frequency sweep 3 % modification at reference temperature of 40 °C.

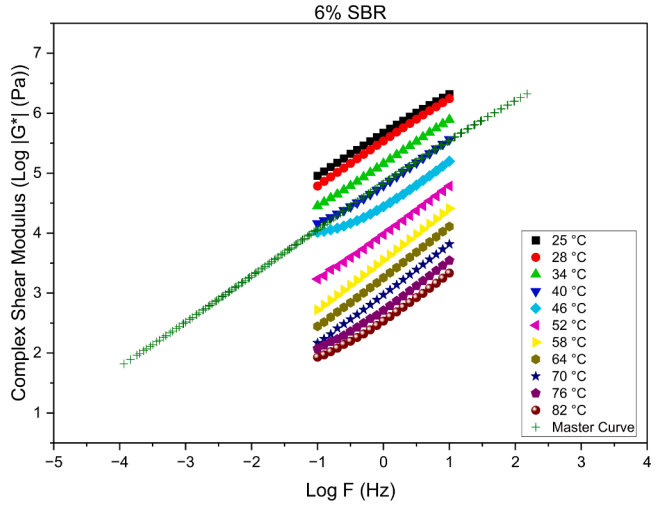

Fig. 6. Frequency sweep for 6 % modification at reference temperature of 40 °C.

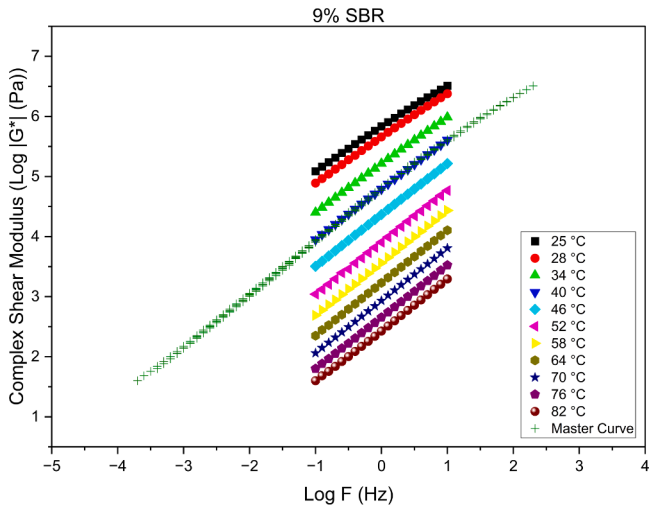

Fig. 7. Frequency sweep for 9 % modification at reference temperature of 40 °C.

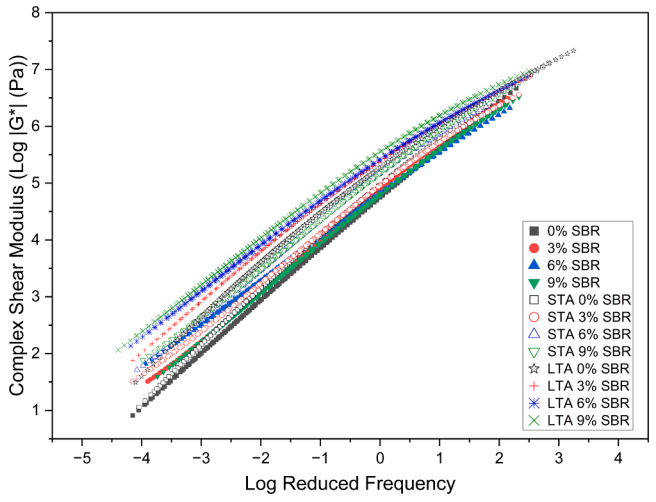

Fig. 8. Effect of SBR dosages (%) and ageing on complex shear modulus master curve for modified and unmodified binders at a reference temperature of 40 °C.

Table 5
(WLF)constants on the effect of SBR dosages (%).

Binder	C1	C2	R^2
0 % SBR	15.043	150.000	0.980
0 % SBR STA	11.620	112.622	0.997
0 % SBR LTA	8.335	71.899	0.999
3 % SBR	14.453	150.000	0.972
3 % SBR STA	14.358	150.000	0.975
3 % SBR LTA	14.506	150.000	0.999
6 % SBR	13.679	150.000	0.988
6 % SBR STA	13.878	150.000	0.957
6 % SBR LTA	14.903	150.000	0.996
9 % SBR	12.793	150.000	0.999
9 % SBR STA	14.093	150.000	0.991
9 % SBR LTA	15.941	150.000	0.990

less brittle at low temperatures. This finding has positive implications for the high-temperature performance of SBR, making it a good material for pavements in tropical regions. This is also reflected in the performance grade test results. The observed effects of SBR on the base binder can be attributed to its elastomeric nature, as we observed in the index property section. At low temperatures, the SBR transitions into a solid

state, which makes the bitumen less viscous and allows the SBR elastic network to begin acting and strengthening its elastic response.

This is manifested in the increase of complex modulus and the decrease of phase angle. However, at low temperatures particularly below its softening point, the base binder which accounts for more than 90 % of the modified binder is still very stiff allowing it to dominate the properties of the binder at this stage. The base binder already exhibits a high complex modulus and low phase angle, making the modification effect of SBR less pronounced. As shown in Fig. 9 the phase angle curves of all samples form a single peak, indicating that the phase angle increases slowly with an increase in temperature and then decreases rapidly in the higher temperature region. This trend reflects the combined effect of the SBR and base binder, as explained in the temperature sweep.

4.3.2. Black space diagram

The black space diagrams summarise the rheological behaviour of the modified and unmodified bitumen. The diagram depicts the complex shear modulus against the phase angle, with the frequency and temperature parameters eliminated [13]. As presented in Fig. 10 the black space diagram curves of SBR modified bitumen shifted towards lower values of phase angles, and a higher complex modulus, with 6 % having the highest stiffness and the lowest phase angle, indicating an increase in elasticity and stiffness.

4.3.3. Cole–cole diagram

The cole-cole diagrams provide critical insights into the viscoelastic behaviour of bitumen, modified or alternative binders, highlighting their performance characteristics [13]. As shown in Fig. 11, the SBR-modified samples exhibited the highest values of loss and storage modulus indicating SBR's ability to enhance stiffness and elasticity across a wide temperature range. This is an indication of the SBR, making it the most effective modifier for applications that require high-performance mechanical properties. As shown in Fig. 12, the curve for the 6 % modification was more inclined to the right, indicating a superior elastic response and a lower viscous response.

4.3.4. Effect of the modification on the rutting parameter

Figs. 13 and 14 summarises the PG high-temperature assessment results for unaged and RTFO bitumen samples before and after modification at 52 °C, 58 °C, 64 °C, 70 °C, and 76 °C, covering the critical range for pavement performance.

The unmodified bitumen exhibited a high G*/sin(δ) value at the lower temperatures, indicating good resistance to rutting, but failed at

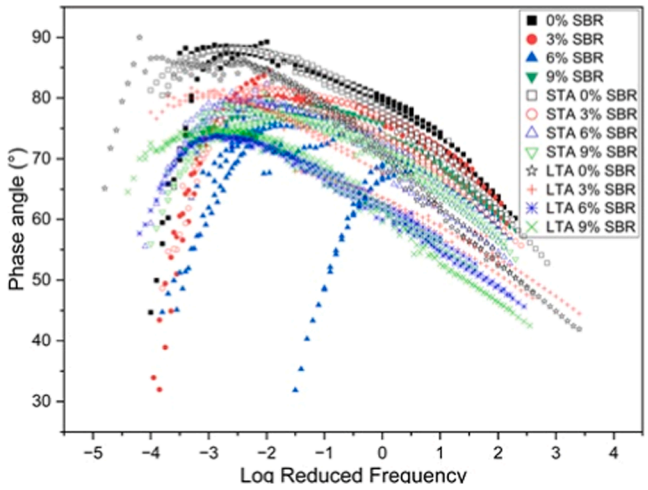

Fig. 9. Effect of SBR dosages (%) and ageing on phase angle master curve for modified and unmodified binders at a reference temperature of 40 °C.

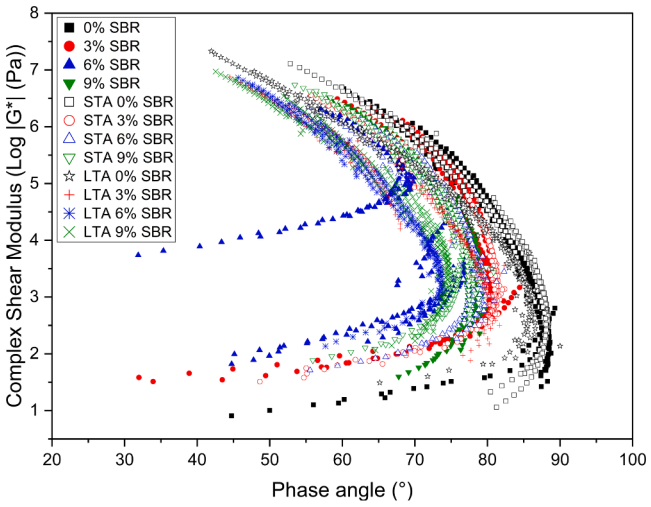

Fig. 10. Effect of SBR dosages (%) and ageing of black space diagram.

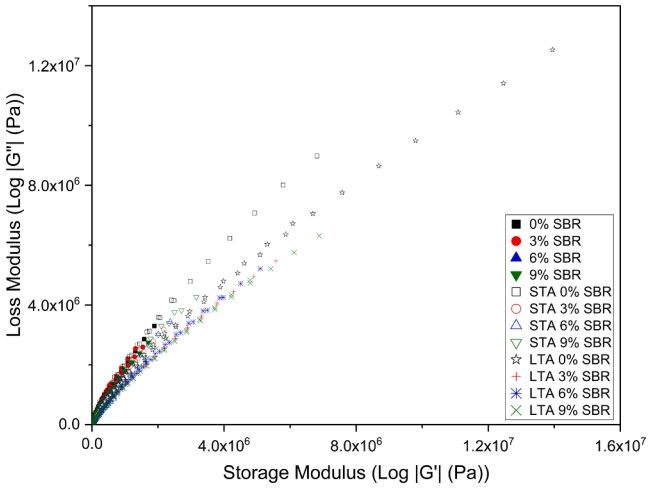

Fig. 11. Effect of SBR dosages (%) and ageing log-log scale of cole-cole diagram.

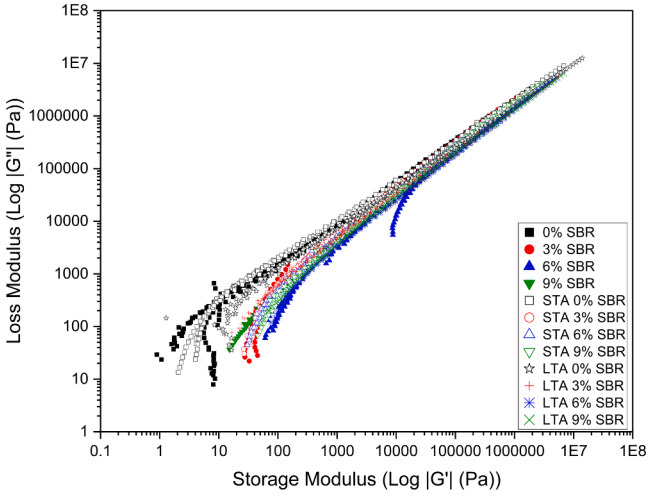

Fig. 12. Linear scale of cole-cole diagram for binder and modified binders at different ageing conditions.

61.52 °C, and improved after short-term ageing. On the other hand, the

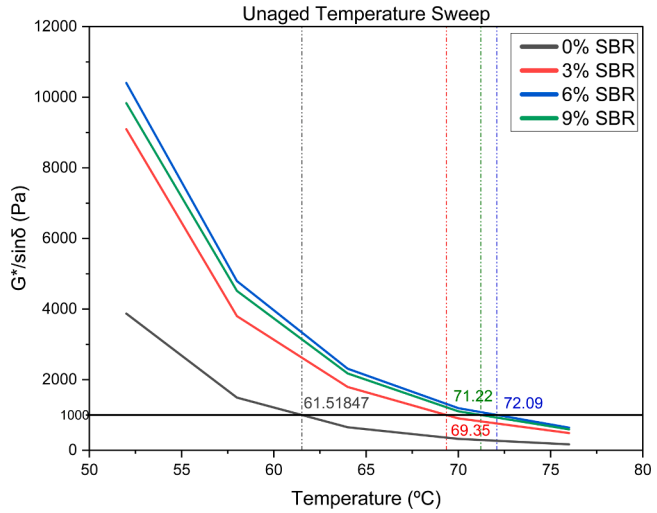

Fig. 13. High temperature performance assessment of the different SBR modifications.

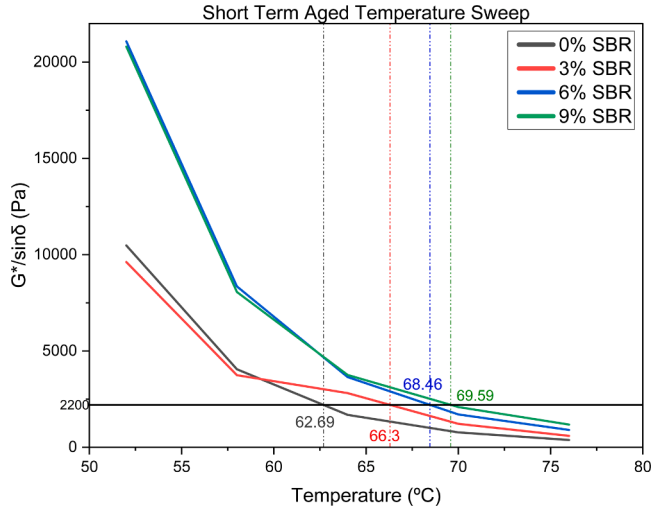

Fig. 14. High temperature performance assessment of the different SBR modifications.

modified bitumen exhibited a superior G*/sin(δ) value across every temperature and extending the binders fail temperature up to 72.09 °C, at 6 % SBR modification and 69.59 °C at 9 % SBR modification for the aged samples. This makes it a good candidate for pavement construction in tropical regions where the average pavement temperature is between 45 °C and 55 °C.

4.4.5. Effect of the modification on the elastic recovery and non-recoverable creep compliance

The modified and unmodified bitumen were evaluated using %R and Jnr at stress levels of 0.1 kPa and 3.2 kPa. A higher %R and a lower Jnr indicate a greater resistance to permanent deformation (rutting) according to the AASHTO M332 standard [59]. Table 6 presents how asphalt binders can be categorised based on their Jnr3.2 and Jnr diff values into four traffic load and volume categories: standard traffic (S Grade), heavy traffic (H Grade), very heavy traffic (V Grade), and extremely heavy traffic (E Grade).

The additional indices obtained from the MSCR test are presented in Table 7 to Table 10 and providing a comparative analysis of the high-temperature performance of the various percentages of SBR-modified binders. At 64 °C, the control binder (0 % SBR) exhibited a non-recoverable creep compliance (Jnr) of 0.590kPa^{-1} at 0.1 kPa and 0.697kPa^{-1} at 3.2 kPa, with a very low percent recovery of 2.79 % and 0 %, respectively.

This indicates a predominantly viscous response with minimal elastic recovery under repeated loading. Upon modification with 3 % SBR, the Jnr values decreased to 0.374kPa^{-1} at 0.1 kPa and 0.537kPa^{-1} at 3.2 kPa which represent reductions of approximately 36.6 % and 23.0 % respectively, as compared to the control binder. At the same time, the percent recovery increased to 14.87 % at 0.1 kPa, although the recovery at the higher stress level remained relatively low (0.32 %). This indicates the beginning of polymer network formation that improves the binder's elastic response.

It is evident that an improvement was observed at 6 % SBR having the Jnr values decreased to 0.321kPa^{-1} at 0.1 kPa and 0.487kPa^{-1} at 3.2 kPa. This corresponds to the reductions of approximately 45.7 % and 30.1 % relative to the control binder. In addition, the percent recovery increased to 18.96 % at 0.1 kPa and 1.39 % at 3.2 kPa, which shows that there is a stronger elastic response and improved resistance to permanent deformation. At this dosage, the binder achieved an Extreme traffic (E) grade demonstrating its suitability for pavement subjected to high traffic conditions.

At 9 % SBR modification, the Jnr values increased to 0.342kPa^{-1} at 0.1 kPa and 0.497kPa^{-1} at 3.2 kPa which is 6.6 % and 2.1 % increment respectively as compared to the 6 % SBR binder. However, it was observed that the percent recovery improved to 18.45 % at 0.1 kPa and 1.71 % at 3.2 kPa respectively. This enhancement in elastic recovery is minimal despite the slight increase in creep compliance. This behaviour suggests that a 6 % SBR dosage is optimal for minimising permanent deformation. The further additional polymer content at 9 % SBR may lead to increased stress sensitivity or partial polymer saturation which may result in poor performance of the binder. Nevertheless, the 9 % SBR binder still maintained an Extreme traffic (E) grade, confirming its high-performance capability under severe loading conditions.

In summary, the 6 % and 9 % SBR contents showed the best high-temperature performance among the tested binders. The 3 % SBR-modified binder also displayed increased resistance to deformation and improved recovery compared with the unmodified binder.

4.5. LAS discussions on the modification performance

Fatigue evaluation was performed on the base binder and the SBR modified binder to assess their durability and performance, and in the subsequent sections, the LAS method is described.

4.5.1. Effect of modification on the performance predictions

The LAS method [50] is based on the visco-elastic continuum damage (VECD) approach to predict binder fatigue life as a function of the

Table 6
AASHTO M332 Pavement asphalt grades [59].

Designation	Test Temperature	Requirements	
		Jnr3.2	Jnr diff.
Standard Traffic Loading (S)	PG high temperature	≤ 4.5 kPa	≤ 75 %
Heavy Traffic Loading (H)	PG high temperature	≤ 2.0 kPa	≤ 75 %
Very Heavy Traffic Loading (V)	PG high temperature	≤ 1.0 kPa	≤ 75 %
Extreme Traffic Loading (E)	PG high temperature	≤ 0.5 kPa	≤ 75 %

Table 7
MSCR indices for different SBR modifications at 64 °C.

Binder Type	Jnr 0.1	Jnr 3.2	Jnr diff.	%R 0.1	%R 3.2	Designation
0 % SBR	0.590	0.697	18.186	2.790	0.000	V Grade
3 % SBR	0.374	0.537	43.502	14.868	0.315	V Grade
6 % SBR	0.321	0.487	51.913	18.962	1.390	E Grade
9 % SBR	0.342	0.497	45.482	18.454	1.705	E Grade

Table 8
MSCR indices for different SBR modifications at 70 °C.

Binder Type	Jnr 0.1	Jnr 3.2	Jnr diff.	%R 0.1	%R 3.2	Designation
0 % SBR	1.350	1.509	11.791	0.416	0.000	H Grade
3 % SBR	0.922	1.209	31.110	6.254	0.000	H Grade
6 % SBR	0.696	1.046	50.274	14.704	0.002	H Grade
9 % SBR	0.727	1.078	48.298	14.525	0.055	H Grade

Table 9
MSCR indices for different SBR modifications at 76 °C.

Binder Type	Jnr 0.1	Jnr 3.2	Jnr diff.	%R 0.1	%R 3.2	Designation
0 % SBR	2.745	3.029	10.332	0.000	0.000	S Grade
3 % SBR	2.005	2.494	24.393	1.896	0.000	S Grade
6 % SBR	0.981	1.504	53.420	13.192	0.000	H Grade
9 % SBR	1.090	1.960	79.931	24.225	0.000	-

Table 10
MSCR indices for different SBR modifications at 82 °C.

Binder Type	Jnr 0.1	Jnr 3.2	Jnr diff.	%R 0.1	%R 3.2	Designation
0 % SBR	5.166	5.737	11.051	0.000	0.000	-
3 % SBR	3.909	4.750	21.492	0.032	0.000	-
6 % SBR	1.393	2.741	96.813	18.922	0.000	-
9 % SBR	2.771	3.758	35.619	5.116	0.000	S Grade

strain level of asphalt materials. The LAS test was performed on the base binder and the SBR modified binder to evaluate the fatigue performance of the binders [51]. The developed Fatigue models for the base binder and the SBR modified binder based on (VECD) analysis are shown in Table 11. At a strain level of 2.5 %, the fatigue life of the 6 % SBR-modified binder increases by 47 % compared with the unmodified binder. However, at strain levels of 5 % and 15 %, the fatigue life of the 6 % SBR-modified binder increases by 51 % and 58 %, respectively, compared with the unmodified binder. The results suggest that the addition of SBR could improve the fatigue resistance of asphalt binders at both high and low strain levels, as shown in the fatigue lines in Fig. 17 This also suggests that SBR is suitable for enhancing the fatigue resistance of asphalt binders under both high and low traffic loads.

In general, the fatigue life at all the strain levels was improved, and 9 % SBR modified binder had the highest fatigue life at a strain level of 2.5 % and 5 %. However, at 15 % strain level, the 6 % modified SBR had the highest among all the modifications compared to the base binder. Though as shown in the Fig. 17 at low strain levels, as the SBR percentages are increased there was significant improvement in the fatigue life however as the strain level increases the improvement becomes insignificant beyond 6 % modification as presented in Table 11. Hence, considering cost and performance, one could deduce that 6 % is the optimal dosage for the modification. For comparison purposes, the N_f values at 2.5 %, 5 %, and 15 % strain levels are given in Table 11.

4.5.2. *Effect of modification on stress-strain response*

In this study, the LAS tests were used to evaluate the effect of SBR modification on the fatigue resistance of asphalt binders Fig. 15 presents the stress-strain curves obtained from the LAS tests. It is evident that, as

Table 11
Fatigue parameters of binders and modified binders.

Binder Type	N_f at the strain level of			$N_F = A[\gamma_{max}]^{-B}$
	2.5 %	5 %	15 %	
0 % SBR	74,675	3404	25	$4.427E^{+06}[\gamma_{max}]^{4.455}$
3 % SBR	130,877	5550	37	$8.536E^{+06}[\gamma_{max}]^{4.560}$
6 % SBR	158,244	6602	43	$1.055E^{+07}[\gamma_{max}]^{4.583}$
9 % SBR	180,124	7093	42	$1.296E^{+07}[\gamma_{max}]^{4.666}$

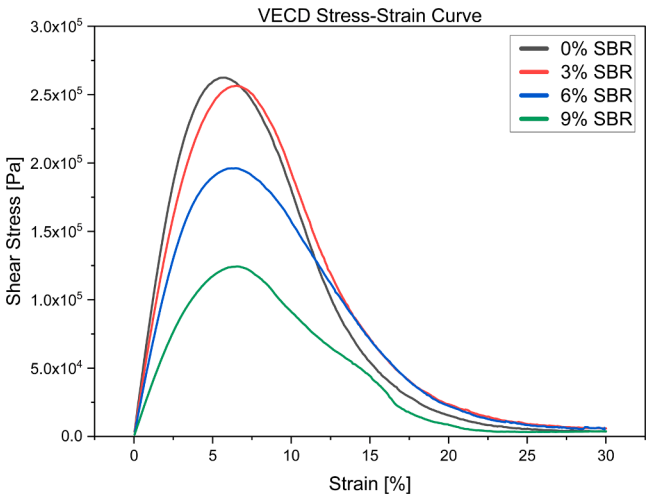

Fig. 15. VECD stress-strain curve for binder and modified binders.

the strain increases, the stress in each sample initially rises and then decreases, forming a stress peak indicating that the binder is within the non-linear zone. The maximum stress and corresponding strain values varied among the Petroleum bitumen and various SBR modification samples.

As shown in Table 12 the unmodified binder showed the heighest peak stress faster than the modified binders. On the other hand, 3 % SBR-modified bitumen showed a peak stress close to the base binder but the highest peak strain value. In summary, 3 % SBR-modified binder could be assumed to perform better than 6 % and 9 % modification. It is also observed that 6 % is lower than the 3 % SBR-modified binder, indicating that the fatigue failure process in the SBR-modified binder progresses more slowly than in the unmodified binder at higher strain levels. The results suggest that the addition of SBR can reduce asphalt hardness, making it more prone to deformation. However, this increased flexibility comes at the cost of reduced fatigue resistance at high strain levels. As shown in Fig. 15 the 3 % SBR modified bitumen showed a maximum stress at 6.52 % strain, while 6 % SBR modified bitumen has a maximum stress at 6.21 %, and 9 % SBR modified bitumen has a maximum stress at 6.31 % strain, while the unmodified bitumen has a maximum stress at 5.72 % strain. The sequence of strain at maximum stress, from lowest to highest for modified bitumen, is 6 %, 9 %, and 3 %, as presented in Table 12.The strain and stress at the failure points of the different asphalt samples, determined at the peak, are listed in Table 12.

4.5.3. *Effect of modification on the damage characteristics curves*

The damage characteristics curve is a typical way to characterise the fatigue behaviour of binders, as shown Fig. 16. The material integrity of the binder can be determined at any damage intensity of interest. The damage characteristic curves, derived from LAS tests, illustrate the properties of the base binder and the SBR-modified binder as depicted.

In the case of undamaged samples, the integrity parameter C consistently holds a value of 1, and when the damage parameter approaches zero, the material is completely damaged. At any specified intensity level, a higher C value indicates greater resistance of the material to damage [53]. All the binders attain peak shear stress at different strain amplitudes, and after this point, a gradual decrease in the peak

Table 12
Fatigue failure points of binders and modified binders.

Binder Type	Peak Stress (Pa)	Strain (%)
0 % SBR	262,500	5.72
3 % SBR	256,500	6.52
6 % SBR	196,100	6.21
9 % SBR	175,100	6.31

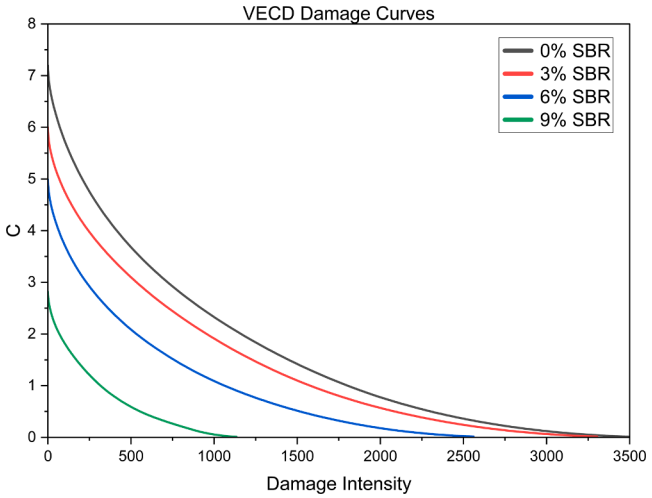

Fig. 16. VECD Damage curve for binder and modified binders.

shear stress and an increase in shear strain were observed. The SBR modified binder shows different damage patterns, although the 3 % binder modification showed similar patterns to the base bitumen. As shown in Fig. 16 as SBR content increases, the damage parameter C decreases more rapidly with damage intensity. This suggests that SBR-modified binders degrade faster under cyclic loading. Although the damage characteristic curves indicate a faster reduction in integrity C with increasing SBR content, the fatigue life results demonstrate improved resistance to cracking. This suggests that the modified binders can tolerate greater accumulated damage before failure, consistent with the enhanced elasticity and strain tolerance imparted by the SBR latex modification. However, the damage characteristic curves are insufficient to give an informed decision on the binder fatigue performance.

4.5.4. Effect of modification on the fatigue failure mechanism

The fatigue life of each asphalt sample was calculated at strain levels of 2.5 %, 5 %, and 15 %. At a strain level of 2.5 %, the fatigue life of the 6 % SBR-modified binder increases by 47 % compared with the unmodified binder. However, at strain levels of 5 % and 15 %, the fatigue life of the 6 % SBR-modified binder increases by 51 % and 58 %, respectively, as compared with the unmodified binder. The results suggest that the addition of SBR could improve the fatigue resistance of asphalt binders at both high and low strain levels, as shown in Fig. 17. However, beyond 6 %, the improvement is minimal as the strain level increases, so cost-wise it would not be economical to modify beyond 6 %. However, the

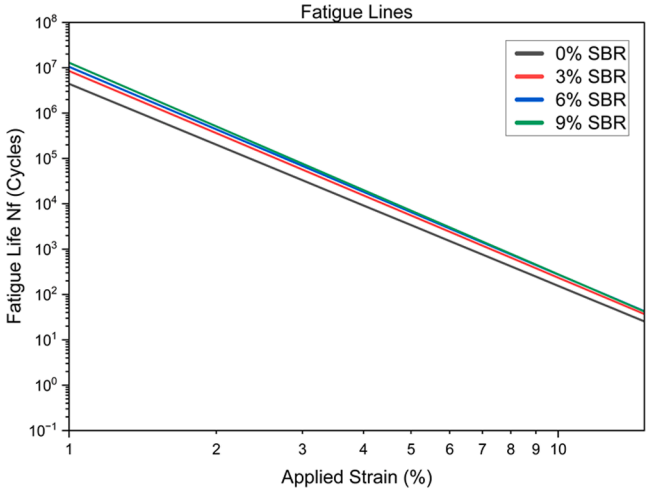

Fig. 17. Fatigue lines of binders and SBR modified binder.

fatigue life of the modified bitumen was also seen to improve when the SBR was increased to 9 %. In general, SBR is suitable for enhancing the fatigue resistance of asphalt binders under both high- and low-traffic loads.

The use of statistical tools to attain the balance in fatigue and in rutting performance of the modified binder as compared to the base binder. This would provide deeper insight into the selection of the optimal SBR dosage in the base binder.

4.5.5. Effect of modification and ageing on the G-R parameter

The G-R Black Space diagram is shown Fig. 18 which was used to evaluate the performance of the base binder and the modified binder in terms of durability and cracking susceptibility. The diagram plots the complex modulus (G*) against the phase angle (δ). Binders within the safe zone are expected to retain adequate flexibility and resistance to thermal or fatigue cracking. Whereas those in the risk zone are considered brittle and prone to cracking under service conditions. The unmodified long-term aged binder (LTA 0 % SBR) lies at the boundary between the transition and risk zones.

This shows that ageing significantly increases binder stiffness while reducing viscoelasticity, thereby raising its vulnerability to cracking. However, the incorporation of Styrene-Butadiene Rubber (SBR) shows a clear improvement as the dosage increases from 3 % to 9 %; the SBR-modified binders shift progressively towards the safe zone, indicating the enhanced elasticity and durability influenced by the polymer. This trend highlights the ability of SBR to offset the embrittlement effect of oxidative ageing by maintaining flexibility and relaxation properties in the binder.

Similarly, the short-term aged (STA) samples are generally closer to the safe zone than long-term aged binders and ageing at this stage is less severe. Nonetheless, adding SBR further consolidates their position in the safe zone, confirming that polymer modification not only enhances the binders under extended ageing but also strengthens early resistance to stiffness. In general, the results demonstrate that SBR modification provides a robust pathway to enhancing cracking resistance and extending pavement service life. Higher SBR dosages (6 % and 9 %) perform particularly well, shifting the binder response firmly towards the safe zone.

4.5.6. Effect of the modification on the storage stability of the optimum modification

The softening point test result for the samples acquired from the 6 % modified binder which was subjected to storage stability test is

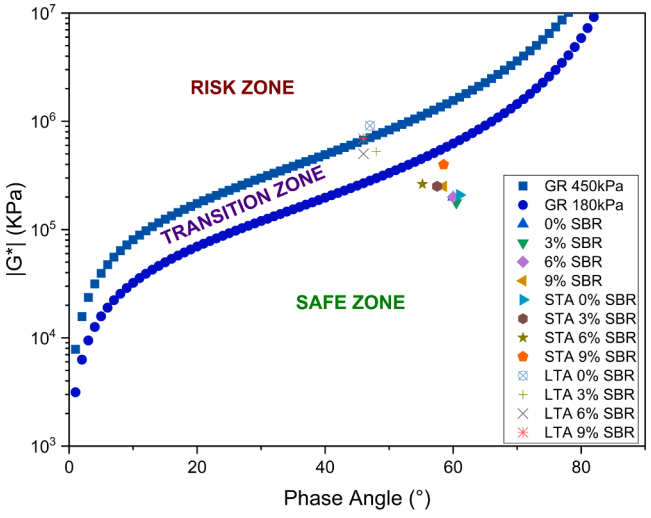

Fig. 18. G-R diagram of binders and SBR modified binder at different ageing conditions.

presented in Fig. 19. The softening point value of the sample obtained from the top of the tube after the storage stability test was slightly lower than that of the sample from the bottom of the tube by a difference of 0.3 °C and a top-to-bottom ratio of 0.99. This indicates that the bitumen modified with SBR would remain uniform and stable during storage and would not affect performance upon use after storage.

Based on the index properties, the storage stability test was conducted only on the 6 % SBR-modified binder. The 6 % dosage was selected because it represents the intermediate (average) modification level among the investigated contents (3 %, 6 %, and 9 %). Given that storage stability in this method is evaluated based on the softening point difference between the top and bottom sections i.e., a relative comparison, it was reasonably assumed that the 6 % binder would provide a representative indication of phase behavior within the studied modification range. Consequently, the result obtained at 6 % was considered enough to infer the compatibility trend of the lower (3 %) and higher (9 %) dosages within the experimental scope.

4.6. Effect of the modification on the binder using statistical analysis

Modified bitumen demonstrates complex rheological properties that are critical in predicting its performance under varying service conditions. To complement the experimental evaluation, statistical tools were employed to better interpret the relationships and underlying patterns among the measured performance indicators.

4.6.1. PCA discussion on the findings from the modification

As shown in Fig. 20 the scree plots presented the eigenvalue values from principal components F1, F2 F3 and F4. It was observed that the eigenvalues gradually reduced from approximately 10 to about 2 for F1 and F2, and then for F3 and F4 tending to zero. This shows that only principal component (F1) and principal component (F1) are adequate to represent the behaviour of the material. The eigenvalue summary is presented in Table 13. The first principal component (F1) accounted for 78.0 % of the total variance, while the second component (F2) explained an additional 15.95 %, giving a cumulative variance of 93.96 % for the first two components. This indicates that the performance of the binders can be effectively described using these two principal axes F1 and F2.

The factor loadings presented in Table 14 reveal that F1 is strongly and negatively associated with variables that represent binder stiffness and elastic recovery, such as fatigue life (-0.958), %Recovery (-0.831), fail temperature unaged (-0.999), softening point (-0.948), G*/sin δ (-0.998) and elastic recovery (-0.990). Conversely, positive correlations are observed with Jnr 3.2 (1.000) and Penetration (1.000). This pattern suggests that F1 primarily differentiates samples based on stiffness and rutting resistance versus softness and compliance.

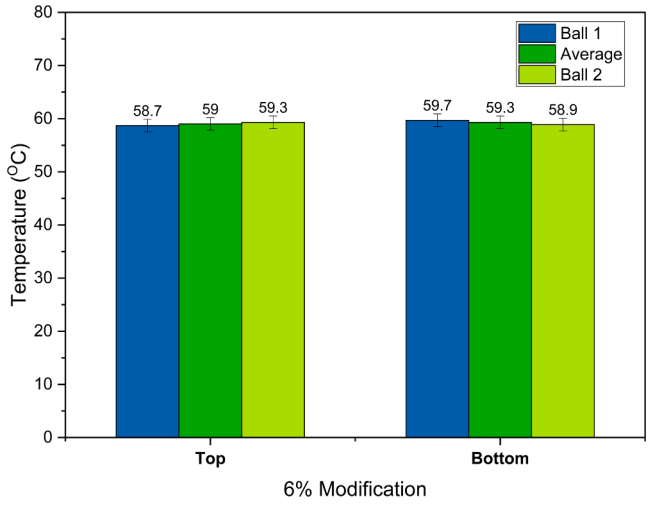

Fig. 19. Storage stability on the effect of SBR 6 % dosage.

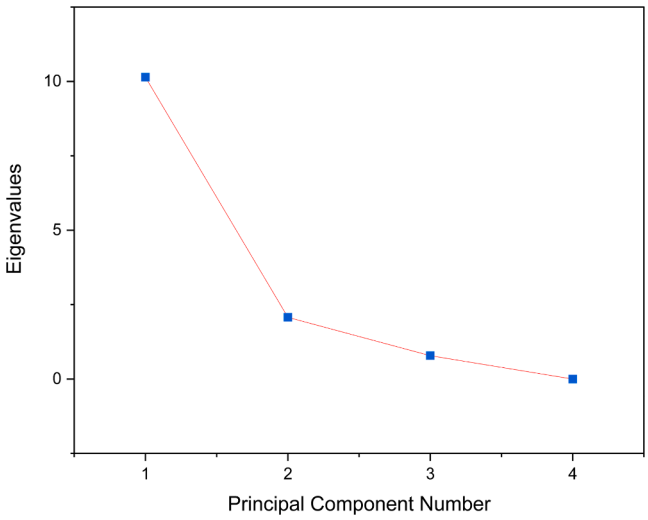

Fig. 20. Eigenvalues scree plot.

Table 13
PCA Eigenvalues.

	F1	F2	F3
Eigenvalue	10.141	2.074	0.785
Variability (%)	78.007	15.953	6.040
Cumulative %	78.007	93.960	100.000

Table 14
Correlations between variables and factors.

Binder property	F1	F2	F3
Fatigue life	-0.958	-0.164	0.235
% Recovery 3.2 (MSCR)	-0.831	-0.515	0.211
Jnr 3.2	1.000	-0.015	0.013
Ageing index (FCF)	0.751	-0.653	-0.103
Ageing index (RF)	0.739	-0.640	0.212
Fail temp unaged (Rutting)	-0.999	0.005	-0.043
Fail temp aged (Rutting)	-0.962	-0.193	0.192
Penetration	1.000	0.022	-0.013
Softening point	-0.948	-0.318	-0.007
G*/sinδ(Rutting)	-0.998	-0.039	-0.044
G*sinδ(Fatigue cracking)	0.217	0.828	0.516
Elastic recovery (ductilimeters)	-0.990	0.074	0.123
Glover rowe	0.760	-0.339	0.554

It was observed that binders with high negative F1 scores exhibit greater stiffness, higher elastic recovery, and improved rutting resistance. In contrast, those with positive scores are softer and more susceptible to deformation. The second component (F2) is dominated by a strong positive loading from G*sin δ (0.828) and negative loadings from the ageing indices (-0.653 for FCF and -0.640 for RF).

This indicates that F2 reflects an ageing response and fatigue susceptibility, with higher positive scores indicating increased fatigue-cracking potential, while negative scores indicate improved ageing resistance. The factor loading plots are presented in Fig. 21.

The factor scores of the individual samples Table 15 further illustrate the influence of SBR modification.

The unmodified 0 % SBR binder recorded a highly positive F1 score (5.361), placing it in the quadrant associated with soft, less-stiff binders with poor rutting resistance. The addition of 3 % SBR shifted the sample slightly towards negative F1 (-0.576) but resulted in a high positive F2 score (2.477), implying a modest improvement in stiffness but a relative increase in the fatigue cracking potential. The binders modified with 6 % SBR (-2.531) and 9 % SBR (-2.254) exhibited strongly negative F1 scores

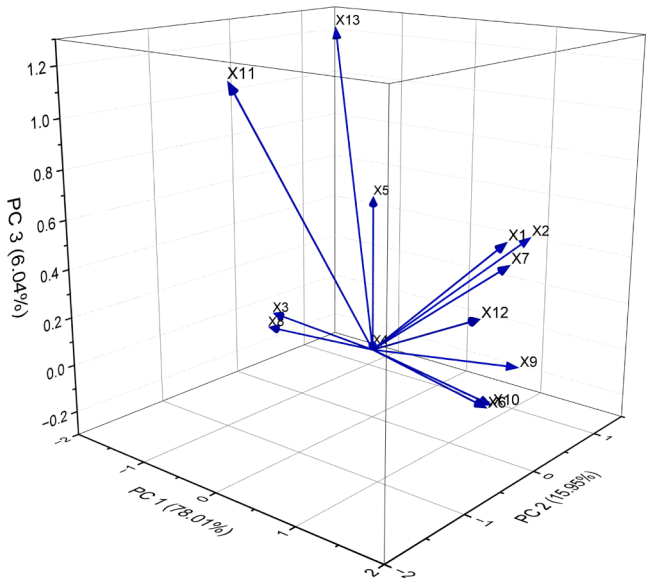

Fig. 21. Factor loading plots.

Table 15
Individual factor scores.

Binder	F1	F2	F3
0 % SBR	5.361	-0.585	-0.026
3 % SBR	-0.576	2.477	-0.078
6 % SBR	-2.531	-1.058	-1.198
9 % SBR	-2.254	-0.835	1.303

with moderately negative F2 scores. This further indicates a significant improvement in stiffness, elastic recovery, ageing resistance, and positioning these binders in the most desirable performance region as shown in Fig. 22.

4.6.2. Effect of the modification on the binder using GRA

GRA was used to rank the overall performance of the binders by combining all measured properties into a single index as shown in Table 16. Given that the parameters had different units and directions, they were first normalised, as shown in Tables 17 and 18 to make them comparable. GRC were then calculated and presented in Table 18 to know how close each binder is to the ideal value for each property. These coefficients were averaged to obtain the GRG, which was used to rank the binders, as shown in Table 19 6 % SBR (0.843, Rank 1), 9 % SBR

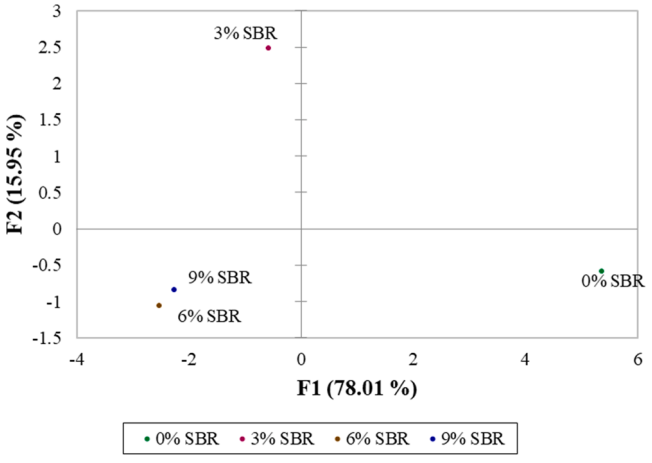

Fig. 22. Individual factor score plot.

Table 16
Performance indicators of base binder and modified binders.

Performance indicators	0 % SBR	3 % SBR	6 % SBR	9 % SBR
Fatigue life	74,675.00	130,877.00	158,244.00	180,124.00
% Recovery 3.2 (MSCR)	0.00	0.32	1.39	1.71
Jnr 3.2	0.70	0.54	0.49	0.50
Ageing index (FCF)	5.38	2.24	3.67	3.31
Ageing index (RF)	2.53	1.24	1.64	1.90
Fail temp unaged (Rutting)	61.52	69.35	72.09	71.22
Fail temp aged (Rutting)	62.69	66.30	68.46	69.59
Penetration	66.00	55.70	52.00	52.30
Softening point	48.10	52.40	57.80	57.20
G*/sinδ (Rutting)	1491.38	3801.04	4793.39	4513.14
G*sinδ (Fatigue Cracking)	581,659.20	705,416.40	442,178.60	592,014.00
Elastic recovery ductilometer	2.50	57.50	65.00	72.50
Glover rowe	580.02	308.99	267.06	464.10

Table 17
Normalised data of base binder and modified binders.

Performance indicators	0 % SBR	3 % SBR	6 % SBR	9 % SBR
Fatigue life	0.000	0.533	0.793	1.000
% Recovery 3.2 (MSCR)	0.000	0.185	0.815	1.000
Jnr 3.2	0.000	0.762	1.000	0.951
Ageing index (FCF)	0.000	1.000	0.543	0.660
Ageing index (RF)	1.000	0.000	0.309	0.514
Fail temp unaged (Rutting)	0.000	0.741	1.000	0.918
Fail temp aged (Rutting)	0.000	0.523	0.836	1.000
Penetration	0.000	0.736	1.000	0.979
Softening point	0.000	0.443	1.000	0.938
G*/sinδ (Rutting)	0.000	0.699	1.000	0.915
G*sinδ (Fatigue Cracking)	0.470	0.000	1.000	0.431
Elastic recovery ductilometer	0.000	0.786	0.893	1.000
Glover rowe	0.000	0.866	1.000	0.370

Table 18
GRC Scores of base binder and modified binders.

Performance indicators	0 % SBR	3 % SBR	6 % SBR	9 % SBR
Fatigue life	0.333	0.517	0.707	1.000
% Recovery 3.2 (MSCR)	0.333	0.380	0.730	1.000
Jnr 3.2	0.333	0.677	1.000	0.911
Ageing index (FCF)	0.333	1.000	0.522	0.595
Ageing index (RF)	1.000	0.333	0.420	0.507
Fail temp unaged (Rutting)	0.333	0.659	1.000	0.859
Fail temp aged (Rutting)	0.333	0.512	0.753	1.000
Penetration	0.333	0.654	1.000	0.959
Softening point	0.333	0.473	1.000	0.890
G*/sinδ (Rutting)	0.333	0.625	1.000	0.855
G*sinδ (Fatigue Cracking)	0.486	0.333	1.000	0.468
Elastic recovery ductilometer	0.333	0.700	0.824	1.000
Glover rowe	0.333	0.789	1.000	0.443

Table 19
GRG of base binder and modified binders.

Sample	GRG	Rank
0 % SBR	0.396	4
3 % SBR	0.589	3
6 % SBR	0.843	1
9 % SBR	0.807	2

(0.807, Rank 2), 3 % SBR (0.589, Rank 3), and 0 % SBR (0.396, Rank 4). This clearly shows that SBR modification improves overall performance, with the best results achieved at 6 % and 9 %. The close GRG values

between 6 % and 9 % suggest that beyond 6 %, further gains are marginal.

4.6.3. Effect of the modification on the binder using correlation analysis

The correlation heatmap, as presented in Fig. 23 highlights relationships among the binder performance indicators. The abbreviation of the different performance indicators used in the correlation is presented in Table 20. The correlation analysis showed a strong positive cluster among fatigue life, % recovery, fail temperature (Unaged and Aged), G*/sin δ, softening point, elastic recovery, and rutting parameters.

The correlation values exceed 0.90 in most cases, which indicates that binders with higher fatigue life also tend to show greater recovery, higher softening point, and enhanced rutting resistance. This further reflects the reinforcing effect of SBR modification on temperature susceptibility. The Correlation analysis shows that Jnr 3.2 and penetration were strongly and negatively correlated with this group, with correlation values below –0.95. This further gave an insight confirming that binders with higher compliance and penetration are associated with weaker rutting resistance and lower overall performance. The ageing indices FCF and RF exhibited a more complex pattern, with moderate positive correlations with Jnr (0.7591 and 0.7512) and penetration (0.7370 and 0.7213). However, it was observed to have a negative relationship with the rutting and stiffness indicators, ranging from –0.7485 to –0.5465. This suggests that ageing tends to align more with non-recoverable creep compliance and penetrability rather than stiffness and recovery.

The G*sin δ (fatigue cracking) showed weak or negative correlations

Table 20
The abbreviation of the different performance indicators.

Performance Indicator	Abbreviation
Fatigue life	X1
% Recovery 3.2 (MSCR)	X2
Jnr 3.2	X3
Ageing index (FCF)	X4
Ageing index (RF)	X5
Fail temp unaged (Rutting)	X6
Fail temp aged (Rutting)	X7
Penetration	X8
Softening point	X9
G*/sinδ (Rutting)	X10
G*sinδ (Fatigue Cracking)	X11
Elastic recovery ductilometer	X12
Glover rowe	X13

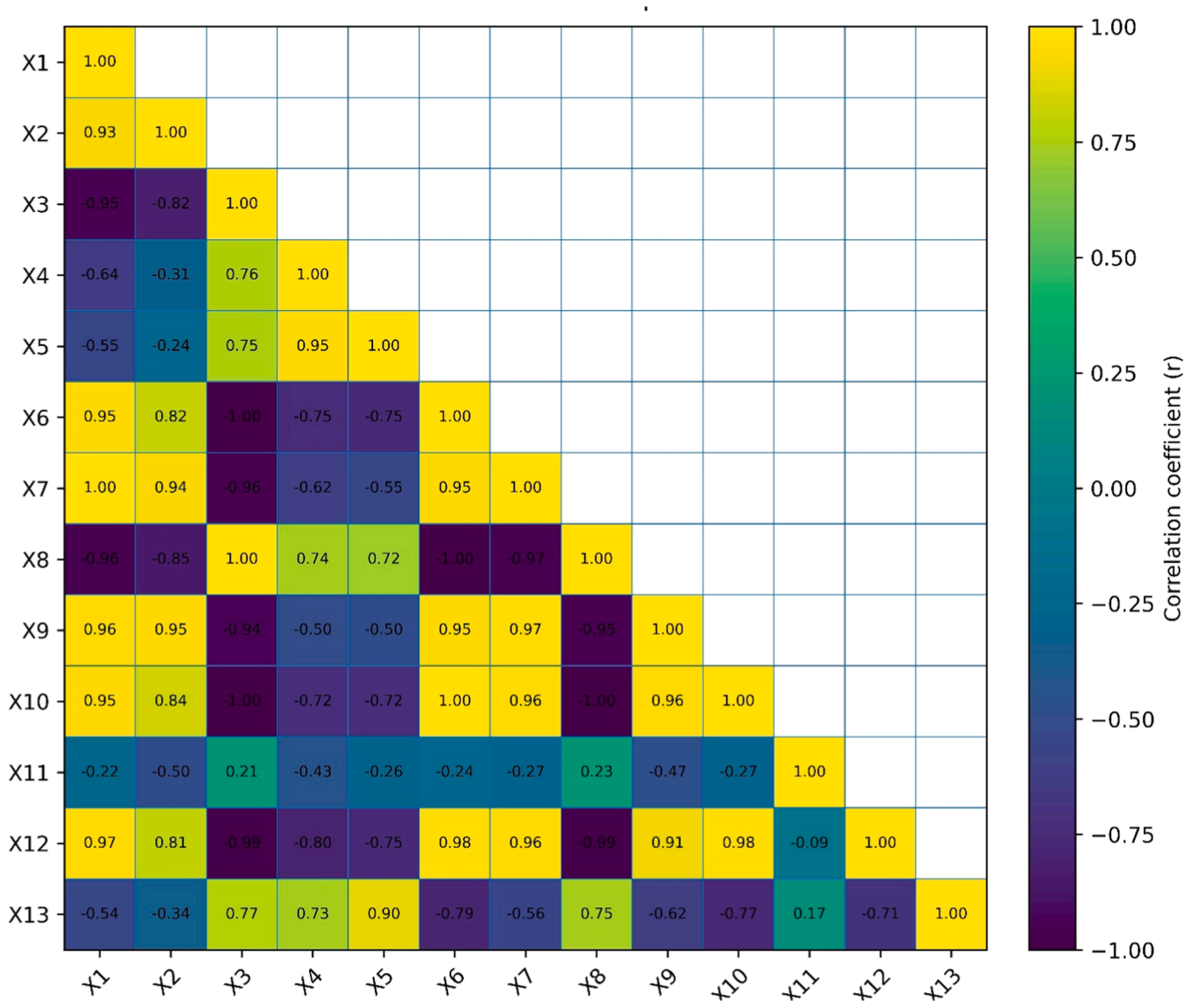

Fig. 23. Heat correlation map.

with most stiff parameters and only moderate positive relationships with ageing indices, indicating that fatigue cracking resistance is influenced differently from rutting resistance. The G-R parameter showed positive relationships with Jnr value of 0.7729 and fatigue ageing indices factor of 0.7348. However, it shows a negative correlation with rutting-parameter G*/sin δ of value –0.7699 and elastic recovery of –0.7095. These results align with the PCA findings in Table 14, where the first principal component separated stiffness and recovery variables from penetration and Jnr. The second component captured the influence of ageing and fatigue indicators. The correlation analysis confirms the same grouping of properties, reinforcing the conclusion that SBR modification shifts the binders towards the cluster of stiffness, recovery, and rutting resistance. It also showed that SBR modification influenced ageing and fatigue behaviors in a separate dimension.

5. Conclusions

This study presents the performance of Styrene-Butadiene-Rubber-modified bitumen at various percentages, 0, 3, 6, and 9 %, for its application in tropical regions as a potential for sustainable pavement construction. Based on the research findings, the following conclusions were drawn.

1. The modifier showed no compatibility problem with the base binder, producing homogeneous blends with no observable phase separation. This further indicates the suitability of SBR as a sustainable modifier that can enhance the performance of asphalt applications in tropical regions.
2. The binder modification using SBR improved the high-temperature performance. The increase in softening point values and reduction in penetration indicate enhanced stiffness and resistance to temperature-induced deformation. The modified binders achieved higher performance grades, indicating suitability for regions with pavement temperatures.
3. The non-recoverable creep compliance from the MSCR results was reduced, and the elastic recovery increased with the modification percentage increase. It further led to the improvement of the SBR-modified binders from very heavy traffic (V Grade) to extreme traffic loading categories (E-grade) at 64 °C under the AASHTO M332 classification. This implies improved rutting resistance when used under tropical conditions.
4. The LAS test showed that SBR addition increased the fatigue life of the base binder by 2.1 %, which is an indication of better resistance to cracking and structural degradation under repeated traffic loading. G–R parameter and thermal ageing analyses revealed that SBR-modified binders retained elasticity and resisted embrittlement after ageing. This contrasts with the control binder, which moves towards the brittle risk zone. This indicates a prolonged service life and reduced need for maintenance.
5. The Statistical analysis using GRA and PCA rated 6 % SBR as the optimum formulation providing the ideal balance between stiffness, elasticity, and ageing resistance. Beyond this level, gains were marginal or slightly offset by reduced fatigue resistance.
6. PC analysis gave an insight into the strong positive cluster observed among fatigue life, % recovery, Fail Temperature, G*/sin δ, softening point, elastic recovery, and rutting parameters, with correlation values exceeding 0.90 in most cases at unaged and aged conditions

In summary, the application of SBR-modified bitumen in tropical regions provides the advantage of extending pavement life compared with unmodified bitumen. In achieving the desired optimum performance, it is argued that 6 % is the optimal dosage as reported in the various empirical and rheological tests.

6. Future recommendations

i. It is recommended that this research should be upscaled from binder-level testing to assess the performance of SBR-modified asphalt concrete, focusing on dynamic modulus, indirect tensile strength, moisture susceptibility, rutting and fatigue test protocols.
ii. It is recommended that the effect of this SBR on alternative binders and new innovative binders, such as bio-oil and natural binders, be studied in view of developing a sustainable pavement material for tropical conditions.
iii. Conduct full-scale field trials of SBR-modified asphalt mixtures in tropical climates to evaluate long-term rutting, cracking, and ageing behavior under real traffic and environmental conditions, and compare results with laboratory-simulated samples.
iv. There is a need to evaluate the adhesion and cohesion characteristics of SBR-modified binders with commonly used aggregates in tropical regions to ensure optimum bond strength and resistance to stripping.
v. There is need to investigate the rejuvenation potential of aged SBR-modified binders and their compatibility with reclaimed asphalt pavement (RAP) to promote a circular economy and sustainable pavement practices.
vi. Conduct a life-cycle cost and carbon footprint analysis comparing SBR-modified and conventional binders to quantify the environmental benefits and long-term savings from extended pavement life.

Declaration of generative AI and AI -assisted technologies in the writing process

During the preparation of this manuscript, the author(s) used ChatGPT and Grammarly to improve the readability, images, and language of the manuscript. After using these tools, the authors reviewed and edited the content as needed and take full responsibility for the content of the published article.

Funding

This research received a grant from the Nigerian Building and Road Research Institute (NBRRI) in Nigeria; the Centre for Advanced Pavement Technology (CAPaT) in NBRRI is acknowledged for providing the study facilities. BASF is acknowledged for providing the polymer modifier and technical support used in this study.

Acknowledgments

This research was supported by Nigerian Building and Road Research Institute (NBRRI), TUDelft, BASF, and Nile University of Nigeria. We gratefully acknowledge the financial, equipment and technical support provided.

CRediT authorship contribution statement

Daniel Akinmade: Writing – review & editing, Supervision, Formal analysis, Data curation. **Adesola Afolabi:** Writing – original draft, Methodology, Investigation, Formal analysis, Data curation, Conceptualization. **Adekunle A. Adeleke:** Writing – review & editing, Supervision, Project administration, Investigation. **Samson Duna:** Writing – review & editing, Supervision, Resources, Project administration, Funding acquisition, Conceptualization. **Mario Sandor:** Resources, Project administration, Funding acquisition, Conceptualization. **Kumar Anupam:** Writing – review & editing, Validation, Supervision, Methodology, Investigation, Formal analysis.

Declaration of competing interest

The authors declare the following financial interests/personal relationships which may be considered as potential competing interests: Akinmade Oluwatosin Daniel reports administrative support, article publishing charges, statistical analysis, and writing assistance were provided by Delft University of Technology. Akinmade Oluwatosin Daniel reports financial support was provided by Center for Advance Pavement Technology (CAPaT) in Nigeria. If there are other authors, they declare that they have no known competing financial interests or personal relationships that could have appeared to influence the work reported in this paper.

Data availability

Data will be made available on request.

References

[1] C. Plati, Sustainability factors in pavement materials, design, and preservation strategies: a literature review, Constr. Build. Mater. 211 (2019) 539–555, https://doi.org/10.1016/j.conbuildmat.2019.03.242.

[2] J.C. Nicholls, Asphalt Surfacings, CRC Press, 1998.

[3] J. Sun, et al., Investigation of the performance and micro-evolution mechanism of low-content thermosetting epoxy asphalt binder towards sustainable highway and bridge decks paving, J. Clean. Prod. 384 (2023) 135588, https://doi.org/10.1016/j.jclepro.2022.135588.

[4] K. O'Reilly, Asphalt: a History, U of Nebraska Press, 2021.

[5] E. Behzadfar, S.G. Hatzikiriakos, Viscoelastic properties and constitutive modelling of bitumen, Fuel 108 (2013) 391–399, https://doi.org/10.1016/j.fuel.2012.12.035.

[6] M.R. Hainin, et al., Performance of modified asphalt binder with tire rubber powder, J. Teknol. (Sci. Eng.) 73 (4) (2015), https://doi.org/10.11113/jt.v73.4275.

[7] C. Traffic, *Manual on uniform traffic control devices*. US Department of Transportation, Fed. Highw. Administation 7 (2009).

[8] P.D. Norton, Fighting traffic: the Dawn of the Motor Age in the American city, Mit Press, 2011.

[9] S. Bitumen, The Shell Bitumen Industrial Handbook, Thomas Telford, 1995.

[10] Á. García, E. Schlangen, M. Van de Ven, Properties of capsules containing rejuvenators for their use in asphalt concrete, Fuel 90 (2) (2011) 583–591, https://doi.org/10.1016/j.fuel.2010.09.033.

[11] G. Polacco, et al., Relation between polymer architecture and nonlinear viscoelastic behavior of modified asphalts, Curr. Opin. Colloid. Interface Sci. 11 (4) (2006) 230–245, https://doi.org/10.1016/j.cocis.2006.09.001.

[12] K. Anupam, et al., A state-of-the-art review of natural bitumen in pavement: underlining challenges and the way forward, J. Clean. Prod. 382 (2023) 134957, https://doi.org/10.1016/j.jclepro.2022.134957.

[13] D. Akinmade, et al., Performance of natural asphalt as a paving material: a laboratory and field evaluation, Case Stud. Constr. Mater. 21 (2024) e03823, https://doi.org/10.1016/j.cscm.2024.e03823.

[14] J. Zhu, B. Birgisson, N. Kringos, Polymer modification of bitumen: advances and challenges, Eur. Polym. J. 54 (2014) 18–38, https://doi.org/10.1016/j.eurpolymj.2014.02.005.

[15] Y.M. Alghrafy, E.-S.M. Abd Alla, S.M. El-Badawy, Rheological properties and aging performance of sulfur extended asphalt modified with recycled polyethylene waste, Constr. Build. Mater. 273 (2021) 121771, https://doi.org/10.1016/j.conbuildmat.2020.121771.

[16] H. Ziari, et al., Mechanical characterization of warm mix asphalt mixtures made with RAP and Para-fiber additive, Constr. Build. Mater. 279 (2021) 122456, https://doi.org/10.1016/j.conbuildmat.2021.122456.

[17] Q. Yang, et al., A review of polymer-modified asphalt binder: modification mechanisms and mechanical properties, Clean. Mater. 12 (2024) 100255, https://doi.org/10.1016/j.clema.2024.100255.

[18] H. Li, et al., Effect of SBS and crumb rubber on asphalt modification: a review of the properties and practical application, J. Traffic Transp. Eng. (Engl. Ed.) 9 (5) (2022) 836–863, https://doi.org/10.1016/j.jtte.2022.03.002.

[19] M. Porto, et al., Bitumen and bitumen modification: a review on latest advances, Appl. sci. 9 (4) (2019) 742, https://doi.org/10.3390/app9040742.

[20] G. Hao, et al., Effect of aging on chemical and rheological properties of SBS modified asphalt with different compositions, Constr. Build. Mater. 156 (2017) 902–910, https://doi.org/10.1016/j.conbuildmat.2017.06.146.

[21] C. Yan, et al., Chemical and rheological evaluation of ageing properties of high content SBS polymer modified asphalt, Fuel 252 (2019) 417–426, https://doi.org/10.1016/j.fuel.2019.04.022.

[22] X. Zhao, et al., Rheological and structural evolution of SBS modified asphalts under natural weathering, Fuel 184 (2016) 242–247, https://doi.org/10.1016/j.fuel.2016.07.018.

[23] S.K. Singh, Y. Kumar, S.S. Ravindranath, Thermal degradation of SBS in bitumen during storage: influence of temperature, SBS concentration, polymer type and base bitumen, Polym. Degrad. Stab. 147 (2018) 64–75, https://doi.org/10.1016/j.polymdegradstab.2017.11.008.

[24] P. Wang, et al., Anti-ageing properties of styrene–butadiene–styrene copolymer-modified asphalt combined with multi-walled carbon nanotubes, Road Mater. Pavement Des. 18 (3) (2017) 533–549, https://doi.org/10.1080/14680629.2016.1181561.

[25] R. Mokoena, et al., African case studies: developing pavement temperature maps for performance-graded asphalt bitumen selection, Sustainability. 14 (3) (2022) 1048, https://doi.org/10.3390/su14031048.

[26] S. Ntramah, et al., Evaluation of selected empirical models for asphalt pavement temperature prediction in a tropical climate: the case of Ghana, Sustainability. 15 (22) (2023) 15846, https://doi.org/10.3390/su152215846.

[27] Y. He, et al., Impacts of ultraviolet irradiation on asphalt binder: a comprehensive review, Int. J. Pavement Eng. 26 (1) (2025) 2472839, https://doi.org/10.1080/10298436.2025.2472839.

[28] N.H. Gapski, et al., Impact of urban surfaces' solar reflectance on air temperature and radiation flux, Sustain. Cities. Soc. 96 (2023) 104645, https://doi.org/10.1016/j.scs.2023.104645.

[29] A. Behnood, M.M. Gharehveran, Morphology, rheology, and physical properties of polymer-modified asphalt binders, Eur. Polym. J. 112 (2019) 766–791, https://doi.org/10.1016/j.eurpolymj.2018.10.049.

[30] Enoyoze, A.P., *Development and evaluation of Crumb rubber-modified binders for high-performance asphalt concrete*. 2025.

[31] N. Saboo, et al., Ranking the rheological response of SBS-and EVA-modified bitumen using MSCR and LAS tests, J. Mater. Civ. Eng. 30 (8) (2018) 04018165, https://doi.org/10.1061/(ASCE)MT.1943-5533.0002367.

[32] A.H. Albayati, et al., Performance evaluation of highly modified asphalt binders using elastomeric and plastomeric polymers, Mech. Time-Depend. Mater. 29 (3) (2025) 73, https://doi.org/10.1007/s11043-025-09811-x.

[33] M. Vamegh, M. Ameri, S.F.C. Naeni, Experimental investigation of effect of PP/SBR polymer blends on the moisture resistance and rutting performance of asphalt mixtures, Constr. Build. Mater. 253 (2020) 119197, https://doi.org/10.1016/j.conbuildmat.2020.119197.

[34] H. Chen, et al., Aging resistance of SBS–SBR composite modified asphalt materials for high altitude and cold regions, Mater. Struct. 55 (7) (2022) 187, https://doi.org/10.1617/s11527-022-02024-5.

[35] F. Wang, et al., Weathering aging resistance in seasonal frozen regions: a comparative study of SBS-and SBR-modified asphalt binders through rheological and morphological characterization, Sci. Rep. 15 (1) (2025) 13625, https://doi.org/10.1038/s41598-025-98396-z.

[36] D. Jin, et al., Performance of rubber modified asphalt mixture with tire-derived aggregate subgrade, Constr. Build. Mater. 449 (2024) 138261, https://doi.org/10.1016/j.conbuildmat.2024.138261.

[37] P. Apostolidis, et al., Evaluation of epoxy modification in bitumen, Constr. Build. Mater. 208 (2019) 361–368, https://doi.org/10.1016/j.conbuildmat.2019.03.013.

[38] M. Liang, et al., Thermo-rheological behavior and compatibility of modified asphalt with various styrene–butadiene structures in SBS copolymers, Mater. Des. 88 (2015) 177–185, https://doi.org/10.1016/j.matdes.2015.09.002.

[39] N. Nciri, N. Kim, N. Cho, New insights into the effects of styrene-butadiene-styrene polymer modifier on the structure, properties, and performance of asphalt binder: the case of AP-5 asphalt and solvent deasphalting pitch, Mater. Chem. Phys. 193 (2017) 477–495, https://doi.org/10.1016/j.matchemphys.2017.03.014.

[40] B. Sengoz, A. Topal, G. Isikyakar, Morphology and image analysis of polymer modified bitumens, Constr. Build. Mater. 23 (5) (2009) 1986–1992, https://doi.org/10.1016/j.conbuildmat.2008.08.020.

[41] L. Shan, et al., Effect of styrene-butadiene-styrene (SBS) on the rheological behavior of asphalt binders, Constr. Build. Mater. 231 (2020) 117076, https://doi.org/10.1016/j.conbuildmat.2019.117076.

[42] J. Tang, H. Wang, M. Liang, Molecular simulation and experimental analysis of interaction and compatibility between asphalt binder and styrene-butadiene-styrene, Constr. Build. Mater. 342 (2022) 128028, https://doi.org/10.1016/j.conbuildmat.2022.128028.

[43] Y. Tian, et al., Comparative investigation on three laboratory testing methods for short-term aging of asphalt binder, Constr. Build. Mater. 266 (2021) 121204, https://doi.org/10.1016/j.conbuildmat.2020.121204.

[44] G. Hao, et al., Property changes of SBS modified asphalt binders during short-term aging and implications on quality management, Constr. Build. Mater. 244 (2020) 118323, https://doi.org/10.1016/j.conbuildmat.2020.118323.

[45] ASTM, D., D5, Standard Test Method for Penetration of Bituminous Materials, American Society for Testing and Materials, USA, 2006.

[46] EN, B., 1427: Bitumen and Bituminous Binders-Determination of the Softening Point: Ring and Ball Method, European Committee for Standardization, Brussels, Belgium, 2015.

[47] ASTM, D., D113. Standard Test Method for Ductility of Bituminous Materials, ASTM, West Conshohocken, PA, USA, 2007.

[48] ASTM, D., 7173; Standard Practice for Determining the Separation Tendency of Polymer from Polymer-Modified Asphalt, American Society for Testing and Materials, West Conshohocken, PA, USA, 2020.

[49] J. Zhang, et al., Roles of recycled oils, polyphosphoric acid and sulfur on chemo-rheological and morphological properties of high-viscosity modified asphalt, Constr. Build. Mater. 371 (2023) 130724, https://doi.org/10.1016/j.conbuildmat.2023.130724.

[50] D. ASTM, Standard Test Method For Effect of Heat and Air On a Moving Film of Asphalt (rolling thin-Film Oven Test, Annual Book of ASTM Standards, USA, 2012.

[51] ASTM, D., 6521-18. Standard Practice for Accelerated Aging of Asphalt Binder Using a Pressurized Aging Vessel (PAV), ASTM International, West Conshohocken, PA, 2018.
[52] T. Wasage, J. Stastna, L. Zanzotto, Rheological analysis of multi-stress creep recovery (MSCR) test, Int. J. Pavement Eng. 12 (6) (2011) 561–568, https://doi.org/10.1080/10298436.2011.573557.
[53] A.S. Shahsamandy, et al., Modeling influence of aging and rejuvenation mechanisms on the recycled asphalt pavement (RAP) binder fatigue life through the linear amplitude sweep test, ACS. Sustain. Chem. Eng. 12 (45) (2024) 16577–16591, https://doi.org/10.1021/acssuschemeng.4c04498.
[54] C. Yan, et al., Proposing a novel double sigmoidal model to fit the master curve for various polymer-modified asphalt, Int. J. Pavement Eng. 24 (2) (2023) 2099852, https://doi.org/10.1080/10298436.2022.2099852.
[55] A. Almusawi, et al., Viscoelastic and fatigue performance of modified bitumen using polymer and bio-based additives: a comparative study, Buildings 15 (3) (2025) 306, https://doi.org/10.3390/buildings15030306.
[56] Kalampokis, S., E. Manthos, and J. Valentin. *Rheological investigation of bio-modified bitumen with two types of bio-oil.* in *# PLACEHOLDER_PARENT_METADATA_VALUE#*. 2025. TU Wien, E230-03 Road Engineering.
[57] TP101, A., Standard Method of Test For Estimating Fatigue Resistance of Asphalt Binders Using the Linear Amplitude Sweep, AASHTO, Washington, DC, USA, 2012.
[58] T. AASHTO, AASHTO TP 101-14. Estimating Damage Tolerance of Asphalt Binders Using the Linear Amplitude Sweep, 2014, pp. 1–7.
[59] M. AASHTO, Standard Specification for Performance-Graded Asphalt Binder Using Multiple Stress Creep Recovery (MSCR), American Association of State Highway and Transportation Officials (AASHTO), Washington, DC, USA, 2014.
[60] A.H. Albayati, et al., Performance assessment of eco-friendly asphalt binders using natural asphalt and waste engine oil, Infrastructures. (Basel) 9 (12) (2024) 224, https://doi.org/10.3390/infrastructures9120224.
[61] K.A. Bohn, L.P. Thives, L.P. Specht, Physical, rheological, and permanent deformation behaviors of WMA-RAP asphalt binders, Sustainability. 15 (18) (2023) 13737, https://doi.org/10.3390/su151813737.
[62] Z. Guo, et al., Development of eco-friendly and high-content rubberized asphalt modified by waste cooking oil desulfurized crumb rubber and waste crumb rubber, Constr. Build. Mater. 447 (2024) 138010, https://doi.org/10.1016/j.conbuildmat.2024.138010.
[63] F. Kaseer, A.E. Martin, E. Arámbula-Mercado, Relationship between rheological indices and cracking performance of virgin, recycled, and rejuvenated asphalt binders and mixtures, Transp. Res. Rec. 2675 (9) (2021) 93–109, https://doi.org/10.1177/03611981211007479.
[64] G. Rowe, G. King, M. Anderson, The influence of binder rheology on the cracking of asphalt mixes in airport and highway projects, J. Test. Eval. 42 (5) (2014) 1–10, https://doi.org/10.1520/JTE20130245.
[65] Y. Li, et al., Assessing pavement characteristics: an in-depth evaluation of waste engine oil and Buton rock asphalt composite modified asphalt and its mixture, Constr. Build. Mater. 451 (2024) 138652, https://doi.org/10.1016/j.conbuildmat.2024.138652.
[66] Osei, A., *Classification of bitumen using chemical and rheological properties.* 2024.
[67] P. Lu, et al., Mix design of asphalt plug joint based on response surface method and grey relational analysis, Int. J. Pavement Eng. 24 (2) (2023) 2032699, https://doi.org/10.1080/10298436.2022.2032699.
[68] P. Cheng, et al., Preparation and performance of bitumen modified by melt-blown fabric of waste mask based on Grey relational and radar chart analysis, Polym. (Basel) 16 (1) (2024) 153, https://doi.org/10.3390/polym16010153.
[69] Z. Li, et al., Research on the correlation between the chemical components and the macroscopic properties of asphalt binder, Mater. (Basel) 18 (3) (2025) 610, https://doi.org/10.3390/ma18030610.
[70] M. Decky, et al., Evaluation of the effect of average annual temperatures in Slovakia between 1971 and 2020 on stresses in rigid pavements, Land. (Basel) 11 (6) (2022) 764, https://doi.org/10.3390/land11060764.
[71] N.G. Specifications, Roads and Bridges, 2, Federal Ministry of Works, Abuja, Nigeria, 1997.